

The scenario of two families of compact stars: burning of hadronic stars

Giuseppe Pagliara

***Dipartimento di Fisica e Scienze della Terra, Universita' di Ferrara &
INFN Ferrara, Italy***



***Nuclear Physics, Compact Stars,
and Compact Star Mergers 2016***
NPCSM 2016, Oct.17-Nov.18, 2016, YITP, Kyoto, Japan



Kyoto 27/10/2016

Outline

-) Under the assumption of absolute stability of strange quark matter: modeling the process of conversion of hadronic stars into quark stars
-) Motivation: two families of compact stars from observations?

Strange quark matter hypothesis

(Bodmer 71- Terazawa 79 - Witten 84)

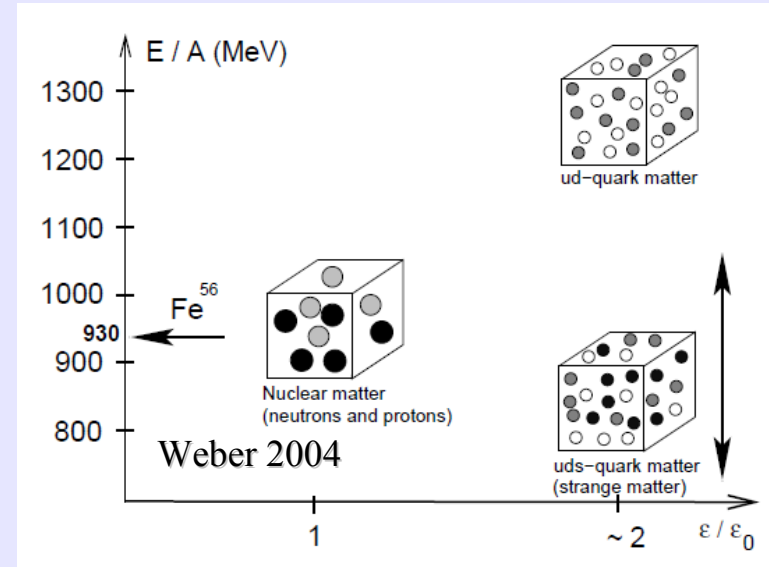
Hyp: “three flavor beta-stable quark matter is more bound than ^{56}Fe .”

Consider three massless quarks: up, down strange. From beta stability the chemical potentials $\mu_d = \mu_s$ implying that the density of strange = density of down. From charge neutrality then the number of up must be = to the number of down. The EoS:

$$P^f = \frac{\nu_f}{24\pi^2} (\mu^f)^4 = \frac{1}{3} \epsilon^f, \quad \rho^f = \frac{\nu_f}{6\pi^2} (\mu^f)^3$$

$$P = (\epsilon - 4B)/3.$$

Where $\nu_f=6$ (color * spin degeneracy)
B is the bag constant of the MIT bag model



Starting with a mixture of up and down quarks, the weak process $u+d \rightarrow u+s$ allows to decrease E/A (a new Fermi sphere opens up) to values smaller than 930 MeV (depending on the values of the parameters)

Birth of quark stars

1) Nucleation of strange quark matter

(not in this talk, see e.g. Iida & Sato 98)

2) Expansion and merging of strange quark matter droplets, formation of a strange quark matter core

(not in this talk, see e.g. Horvath et al. 92)

3) Macroscopic conversion of a hadronic star

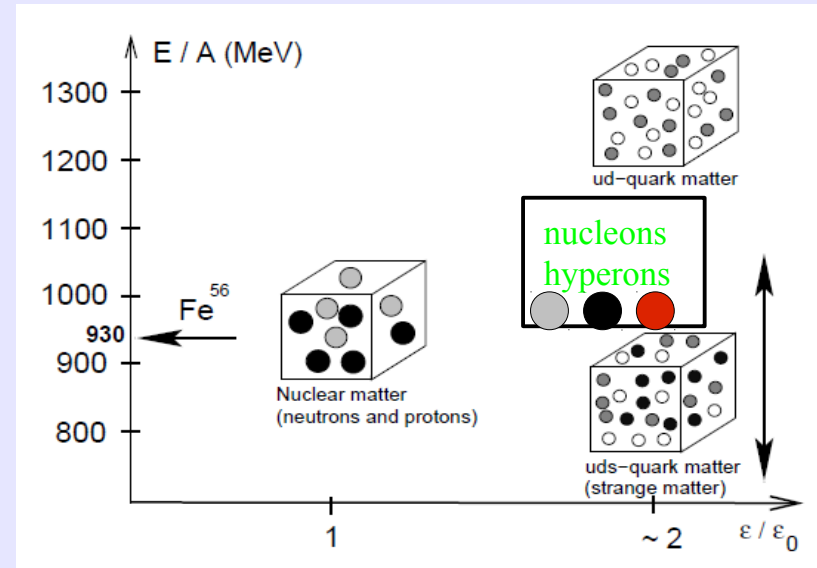
(here!!)

Modeling the conversion

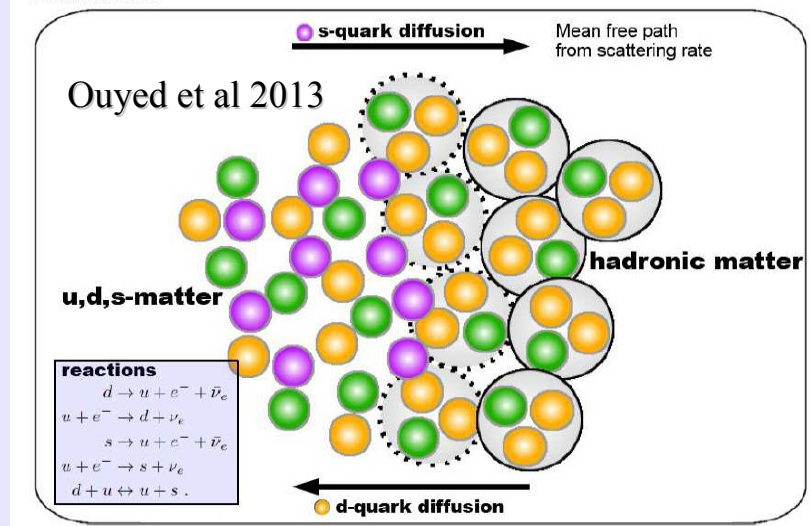
The conversion starts from strange hadronic matter & involves strong interaction (deconfinement) + flavor changing weak interactions $u+d \rightarrow u+s$.

Very complicated to model: deconfinement is a non-perturbative phenomenon.

Olinto 87: let us ignore deconfinement and treat the process as a chemical reaction and borrow the formalism of advection-diffusion-reaction PDE



The Interface



Combustion process

Kinetic theory approach: diffusion of quarks between the two fluids (which are in mechanical equilibrium) and weak interactions

Microphysics: “a” strangeness fraction (n.down-n.strange)/n.baryons

$$D_Q a'' - v_{N \rightarrow Q} a' - \mathcal{R}_Q(a) = 0,$$

$$\mathcal{R}_Q(a) = (\Gamma_{d \rightarrow s} - \Gamma_{s \rightarrow d})/n_Q,$$

Diffusion coefficient:

$$D \simeq 10^{-1} \left(\frac{\mu_f}{300 \text{ MeV}} \right)^{2/3} \left(\frac{T}{10 \text{ MeV}} \right)^{-5/3} \text{ cm}^2/\text{s}$$

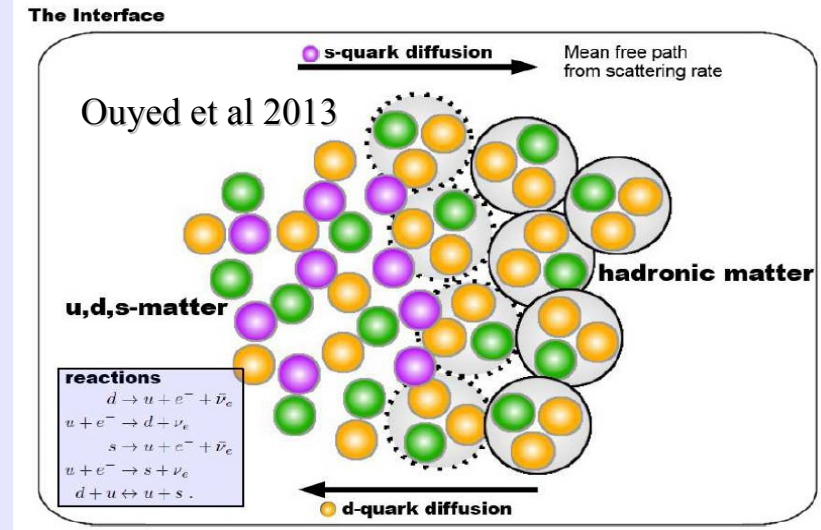
Typical time scale for u+d->u+s:

$$\tau_Q \simeq 1.3 \times 10^{-9} \text{ s } (300 \text{ MeV}/\mu_Q)^5$$

Dimensional analysis:

**1) Typical burning velocity:
 $v \sim \sqrt{D / \tau} \sim 10^4 \text{ cm/s}$ and
 scales as $T^{-5/6}$**

**2) Typical width of the combustion zone:
 $\delta \sim \sqrt{D \tau} \sim 10^{-5} \text{ cm}$ thus
 very small in comparison with
 the size of a star**



This approach does not take into account macroscopic flows driven by pressure/density gradients

Coupling with hydrodynamics

Ouyed 2010: 1D – no gravity – no star!

The 1-D hydrodynamical equations in our case are [24]:

$$\frac{\partial U}{\partial t} = -\nabla F(U) + \mathcal{S}(U) , \quad (1)$$

with variables

$$U = \begin{pmatrix} n_s \\ n_s + n_d \\ n_s + n_d + n_u \\ hv \\ s \end{pmatrix} , \quad (2)$$

and corresponding advective-diffusive terms

$$F(U) = \begin{pmatrix} vn_s + D\nabla n_s \\ v(n_s + n_d) \\ v(n_s + n_d + n_u) \\ hv^2 + P \\ vs \end{pmatrix} , \quad (3)$$

and source terms

$$\mathcal{S}(U) = \begin{pmatrix} -\Gamma_3 + \Gamma_4 + \Gamma_5 \\ -\Gamma_1 + \Gamma_2 - \Gamma_3 + \Gamma_4 \\ 0 \\ 0 \\ -\frac{1}{T} \sum_i \mu_i \frac{dn_i}{dt} \end{pmatrix} . \quad (4)$$

Such a calculation would be impossible in 2 or 3D which are needed to study the possible occurrence of hydrodynamical instabilities.

A similar problem when simulating type Ia SN.

Two possible strategies:

1) Khokhlov 1993:

$$\frac{\partial \rho}{\partial t} = -\nabla \cdot (\rho U) ,$$

$$\frac{\partial \rho U}{\partial t} = -\nabla \cdot (\rho U U) - \nabla P + \rho g ,$$

$$\frac{\partial E}{\partial t} = -\nabla \cdot [(E + P)U] + \rho U \cdot g + \rho \dot{Q} ,$$

$$\frac{\partial f}{\partial t} + U \cdot \nabla f = K \nabla^2 f + R$$

K and R are rescaled to enlarge the width of the combustion zone over several computational cells. It underestimates hydro-instabilities.

2) Calculate the burning velocities profiles from the microscopic kinetic theory model, assume an **infinitely thin combustion layer**.

Hillebrandt 1999 for type Ia SN

Books: Landau, Fluid dynamics.

Ideal-hydro modeling

p : pressure, e : energy density, n : baryon density, $w=e+p$: enthalpy density, $X: (e+p)/n^2$ dynamical volume, T : energy momentum tensor, u fluid four velocity, γ : Lorentz factor, j : number of baryons converted per unit of surface and time.

$$T^{\mu\nu} = (e + p)u^\mu u^\nu - pg^{\mu\nu}$$

$$\partial_\mu (nu^\mu) = 0$$

$$\partial_\mu T^{\mu\nu} = 0$$

$$e = e(p, n)$$

Eqs. of ideal hydrodynamics

Simplifying: let us consider a stationary and 1D physical situation (we consider only the “x” dependence of the fluid variables)

Surface of discontinuity: flame front

$e_1 \ p_1 \ n_1$

fuel

$e_2 \ p_2 \ n_2$

ashes

Ex: from hydrod. (continuity Eqs.):

$$w_1 \gamma_1^2 v_1 = w_2 \gamma_2^2 v_2$$

$$p_1 + w_1 v_1^2 \gamma_1^2 = p_2 + w_2 v_2^2 \gamma_2^2$$

$$n_1 v_1 \gamma_1 = n_2 v_2 \gamma_2 \equiv j$$

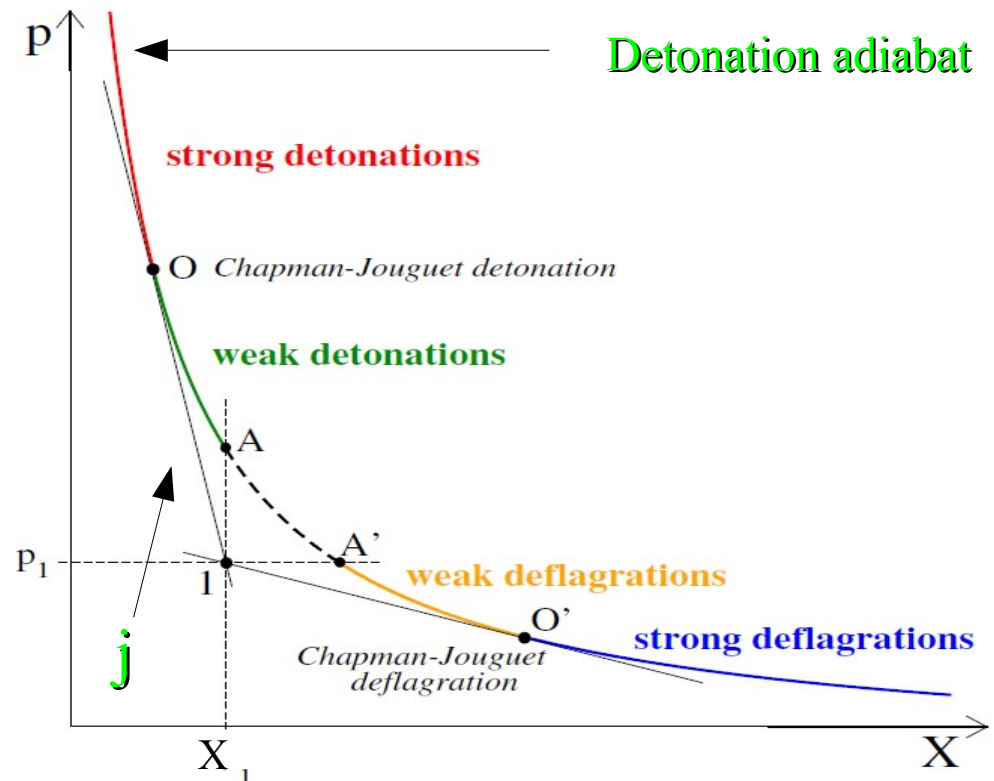
The first two equations can be rewritten as:

$$j^2 = -\frac{(p_2 - p_1)}{(X_2 - X_1)}$$

$$X_2 w_2 - X_1 w_1 = (X_1 + X_2) (p_2 - p_1)$$

This equation defines the so-called “*detonation adiabat*” which is formally identical to a shock adiabat but for the fact that there are two different fluids and thus two different EoSs.

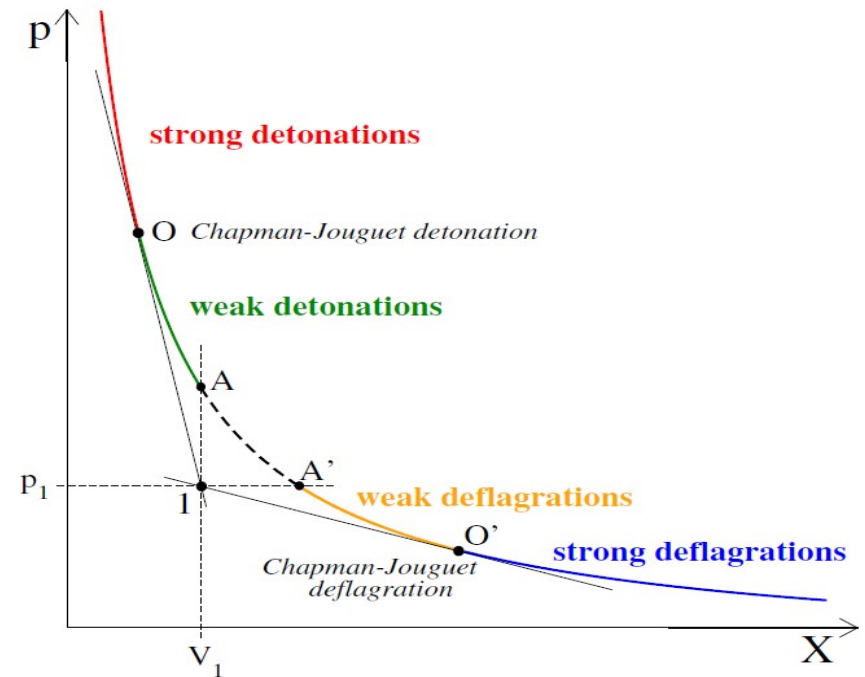
Given the initial state 1, and for a fixed value of j (computed from the microphysics model), the state of fluid 2 is determined.



Qualitatively we can distinguish two different combustion modes:

-) *detonation* (the combustion is driven by a shock wave which heats up the fuel thus catalysing the conversion)
-) *deflagration* (the combustion is driven by the microscopic properties: transport of heat/chemical species and rate of reactions)

By introducing the sound velocities in the two fluids c_i



above	O	$v_1 > c_1, v_2 < c_2$	strong detonation
on	O	$v_1 > c_1, v_2 = c_2$	Chapman – Jouguet detonation
on	AO	$v_1 > c_1, v_2 > c_2$	weak detonation
on	AA'	imaginary flux, no physical significance	
on	A'O'	$v_1 < c_1, v_2 < c_2$	weak deflagration
on	O'	$v_1 < c_1, v_2 = c_2$	Chapman – Jouguet deflagration
below	O'	$v_1 < c_1, v_2 > c_2$	strong deflagration

Several calculations (see Drago 2007) have shown that in the case of burning of hadronic stars, detonations are quite unlikely. The combustion proceeds as a deflagration.

Numerical simulations of Herzog- Roepke 2011:

-) 3+1D code used for SN type Ia simulations
-) Newtonian dynamics + use of an effective relativistic gravitational potential based on TOV (Marek 2006)
-) assume that the combustion proceeds as a deflagration
-) velocity profile taken from Ouyed 2010
-) initial seed: a quark core of 1km which is perturbed with a sinusoidal perturbation of amplitude 0.2 km.
-) EoS: Lattimer-Swesty + MIT bag model
-) 128 or 192 grid cells in each dimension

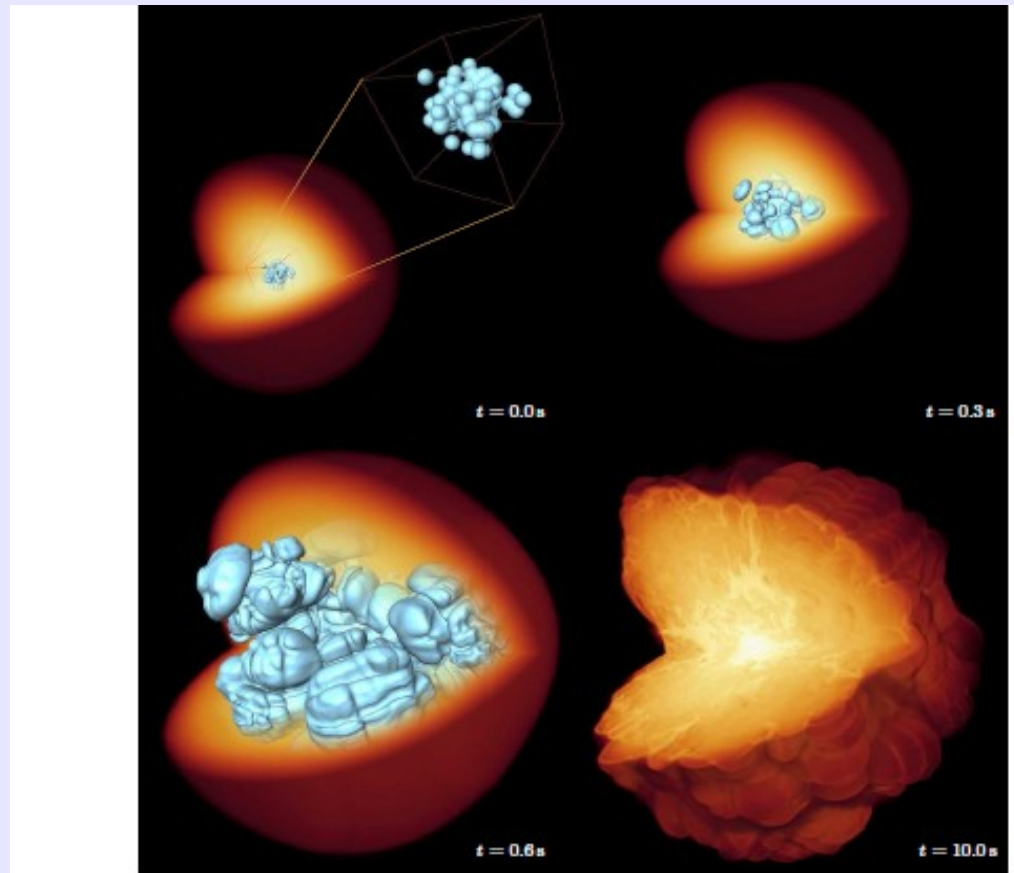
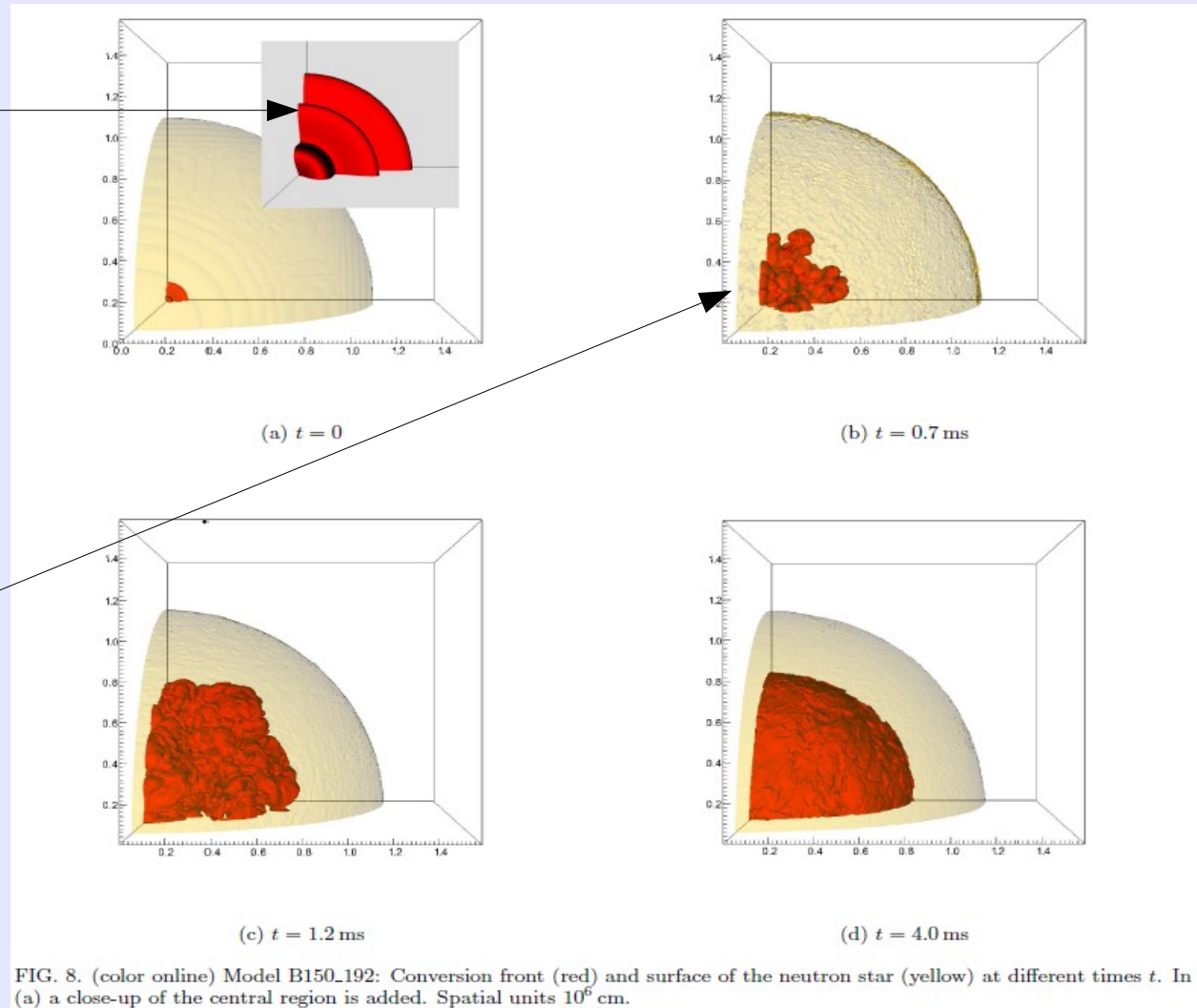


FIGURE 1. Snapshots from a full-star SN Ia simulation starting from a multi-spot ignition scenario. The logarithm of the density is volume rendered indicating the extend of the WD star and the isosurface corresponds to the thermonuclear flame. The last snapshot marks the end of the simulation and is not on scale with the earlier snapshots.

Quark matter seed:
1km +
perturbation on the
density

Mushroom structures
due to
hydrodynamical
instabilities



Time needed for the partial conversion: **few ms, burning velocities substantially increased by Rayleigh-Taylor instabilities.**

-) Effective velocities of conversion increased by several orders of magnitude w.r.t. to the laminar velocities obtained within the purely kinetic theory approach (importance of multiD-hydro)

-) Puzzling result: even if the strange quark matter hyp is assumed to hold true, some material (few $0.1 M_{\text{sun}}$) is left unburnt. The final configuration is similar to a hybrid star. Is this configuration stable?

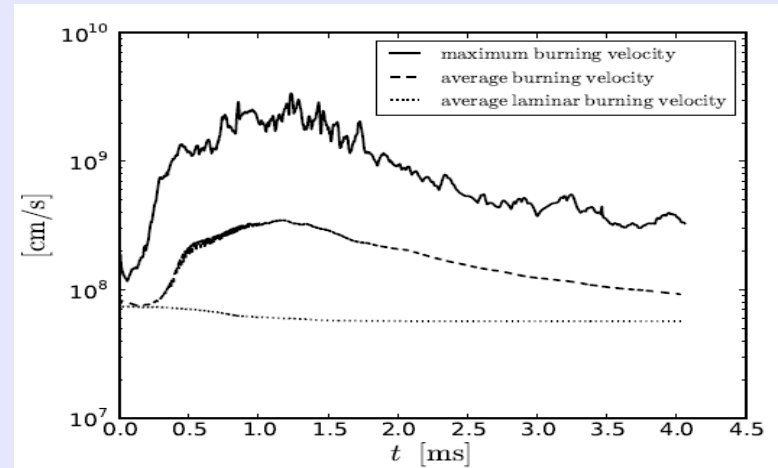
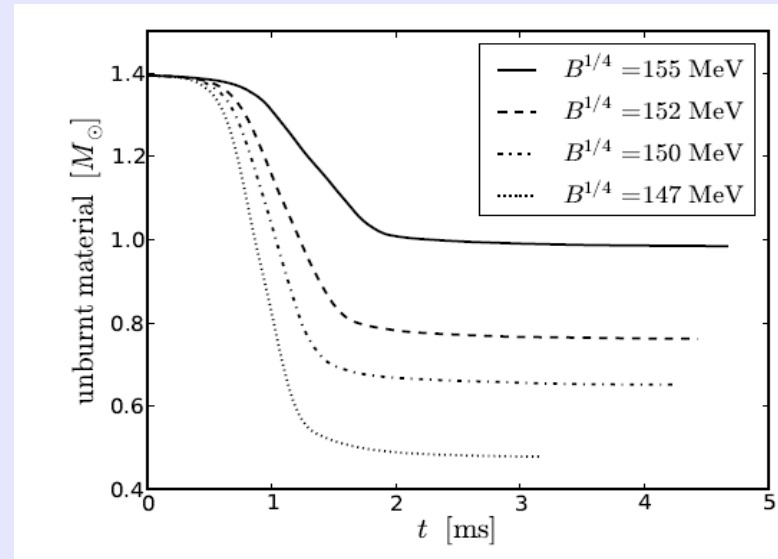


FIG. 7. Burning velocity: Comparison at each timestep of maximum burning velocity, average burning velocity and the underlying average laminar burning velocity. The averages were done over all cells in which burning occurs. Data from the high resolution run with $B^{1/4} = 150$ MeV (model B150_192).



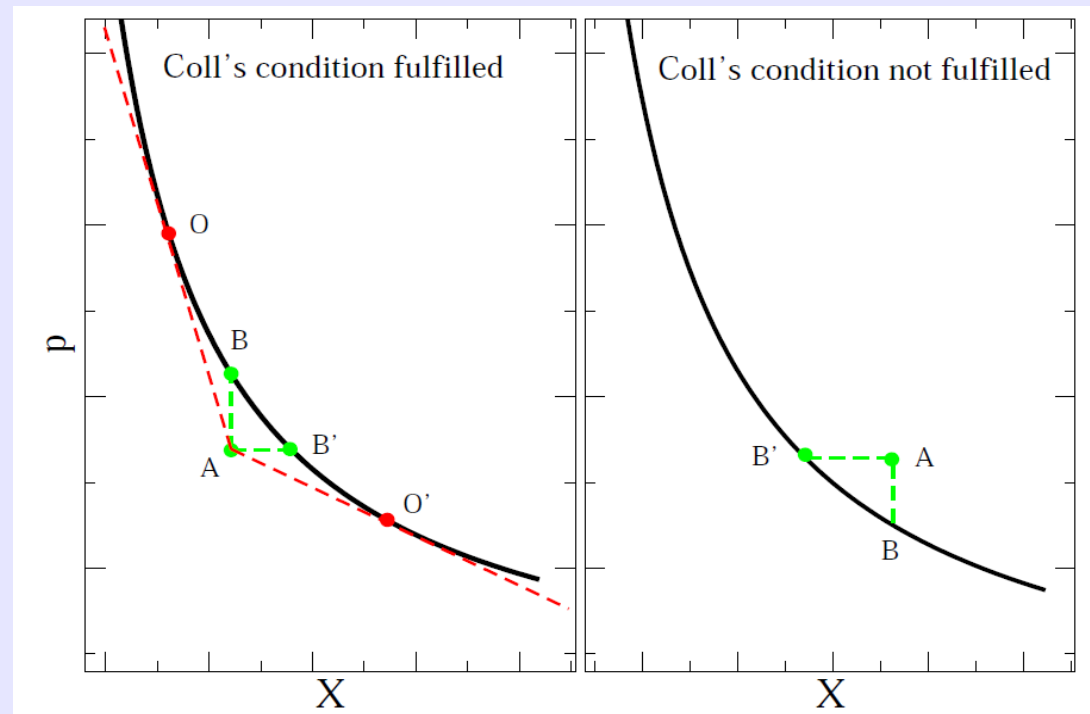
Coll's condition

Coll's condition for “exothermic” combustion (1976), the energy density (or the enthalpy density) of the fuel must be larger than the energy density of the ashes at the same pressure p and dynamical volume X

$$e_1(p, X) > e_2(p, X)$$

$$w_1(p, X) > w_2(p, X)$$

If fulfilled, it implies that the initial point (in the hadronic phase) lies in the region of the p - X plane below the detonation adiabat



Proof

Let us consider an initial state A in hadronic matter (fixed pressure, energy density, baryon density). We consider for simplicity the EoS of massless quark for quark matter

$$e_q = 3p_q + 4B$$

Let us fix the state B of quark matter (which lies on the detonation adiabat) to have the same dynamical volume of the state A. ($X_A = X_B$)

We want to prove that $p_B > p_A$ provided that the Coll's condition holds true.

Let us define:

$$\Delta(p, X) = e_h(p, X) - e_q(p, X) = w_h(p, X) - w_q(p, X) > 0$$

The detonation adiabat reads:

$$\begin{aligned}w_h(p_A, X_A) - w_q(p_B, X_A) &= 2p_A - 2p_B \\e_h(p_A, X_A) + p_A - e_q(p_B, X_A) - p_B + e_q(p_A, X_A) - e_q(p_A, X_A) &= 2p_A - 2p_B \\ \Delta(p_A, X_A) + e_q(p_A, X_A) - e_q(p_B, X_A) &= p_A - p_B \\ \Delta(p_A, X_A) + 3p_A + 4B - 3p_B - 4B &= p_A - p_B \\ \Delta(p_A, X_A) &= 2(p_B - p_A)\end{aligned}$$

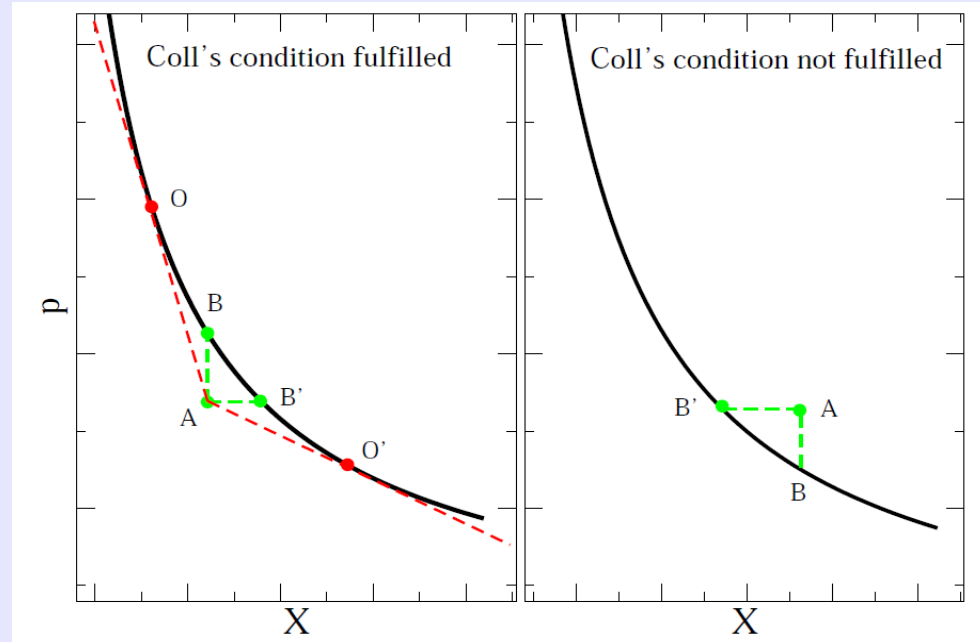
Which implies that if $\Delta > 0$, then $p_B > p_A$ therefore the initial state A lies in the half-plane below the detonation adiabat.

Also for a polytrope it can be shown analitically.

$$p_q = kn_q^\gamma$$

$$e_q = \alpha n_q + p_q / (\gamma - 1)$$

If $e_h(p, X) = e_q(p, X)$ the initial point lies on the detonation adiabat. Moreover, besides the energy density and the pressure, also the baryon density is continuous across the flame front.



If Coll's condition is not fulfilled, there are no Chapman-Jouguet points. No detonation is possible in the star (detonation with no external forces exists only as a Chapman-Jouguet detonation (Landau)).

What about deflagrations? Let us consider the case of a slow combustion (velocity much smaller than the sound velocity, $j \sim 0$ or $p_A \sim p_{B'}$).

In this case the detonation adiabat leads to the conservation of the enthalpy per baryon i.e.

$$(e_A + p_A)/n_A = (e_{B'} + p_A)/n_{B'}$$

Coll's condition implies that

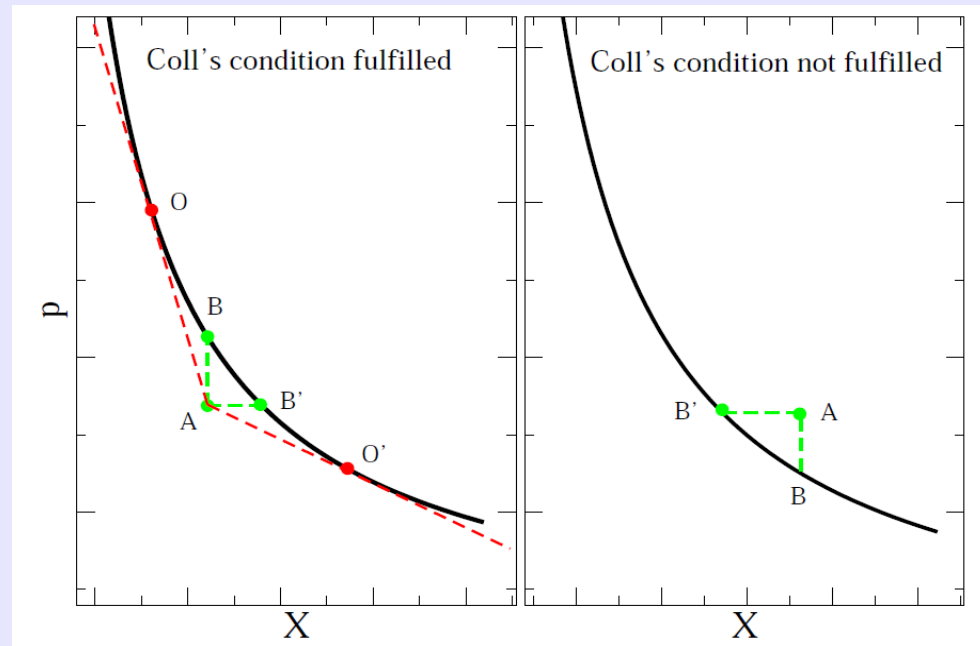
$$X'_B > X_A$$

$$(e_{B'} + p_A)/n_{B'}^2 > (e_A + p_A)/n_A^2$$

$$n_{B'} < n_A$$

$$n_A(e_{B'} + p_A) = n_{B'}(e_A + p_A) < n_A(e_A + p_A)$$

$$e_{B'} < e_A$$

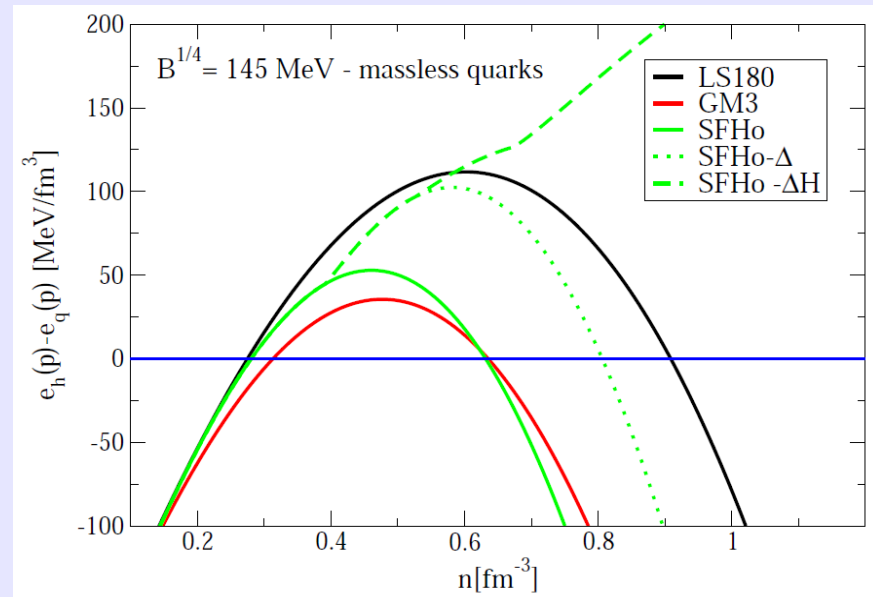


Coll's condition (for the case of a slow combustion) implies that the new phase is produced at a energy density smaller than the one of the fuel: quark matter is lighter than hadronic matter. Inverse density stratification: within the star the gravitational potential and the density gradient point in opposite directions: buoyancy and Rayleigh-Taylor instabilities. If it is violated no instabilities and the velocity of conversion coincides with the (small) laminar velocity (the turbulent eddies stop).

See Drago&Pagliara PRC2015

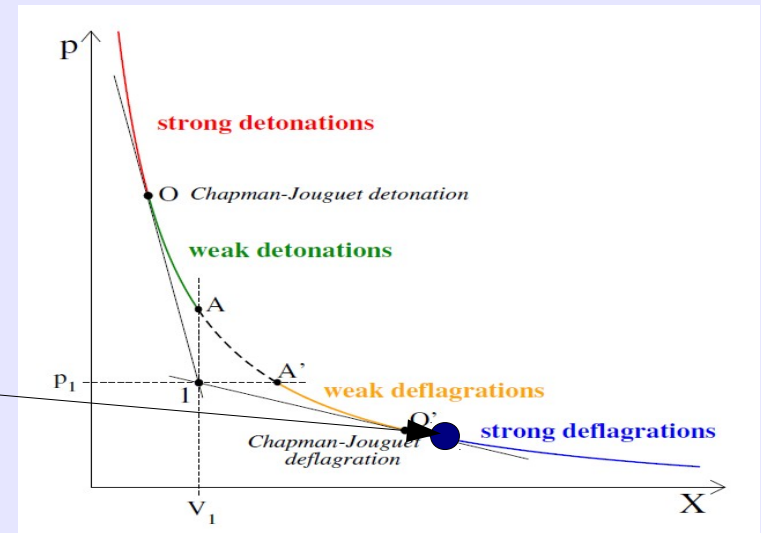
We can define a critical density $\overline{n_h}$ for which $e_h(p, X) = e_q(p, X)$

For different hadronic equations of state it is of $\sim 0.2 - 0.3 \text{ fm}^{-3}$ (example of massless quarks). Note: hyperons enlarge the window of validity of the Coll's condition.



What happens when the combustion front reaches $\overline{n_h}$?

1) At this density, the initial point of the hadronic phase lies on the detonation adiabat:



2) End of turbulent eddies and thus of the fast combustion. Beginning of a **diffusive regime: time scales much longer than the ones of the turbulent regime.**

Fractal model:

$$v_{mh} = v_{lh} (\lambda_{\max} / \lambda_{\min})^{\Delta D}$$

$$\gamma = 1 - \frac{e_2}{e_1}.$$

$$\Delta D = D_0 \gamma^2$$

Fractal dimension ΔD

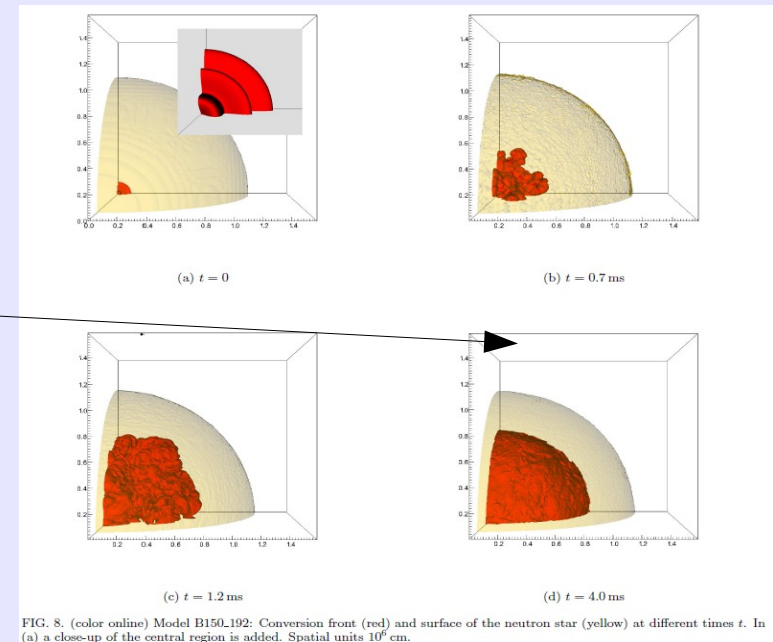
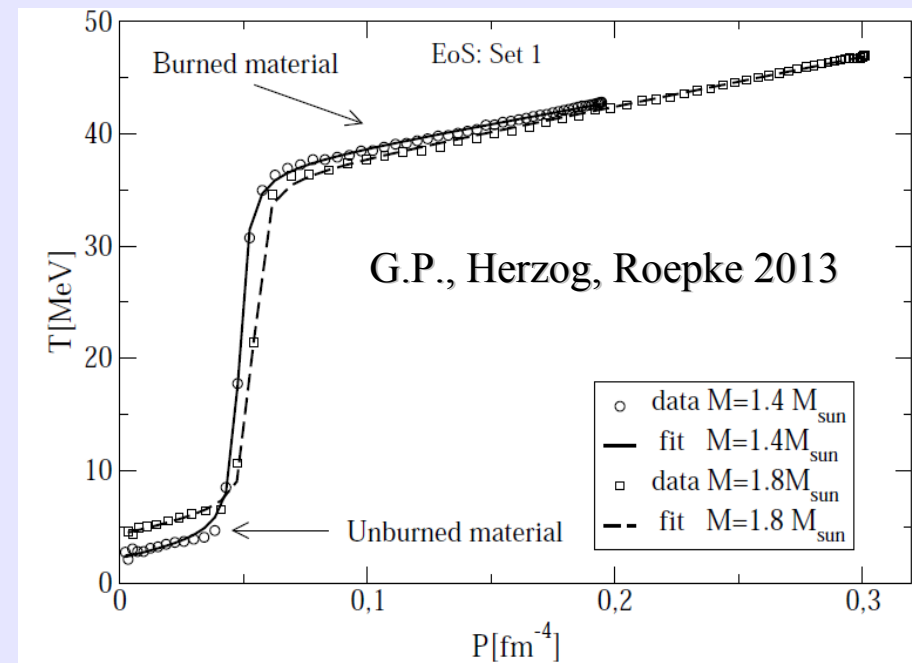


FIG. 8. (color online) Model B150_192: Conversion front (red) and surface of the neutron star (yellow) at different times t . In (a) a close-up of the central region is added. Spatial units 10^6 cm.

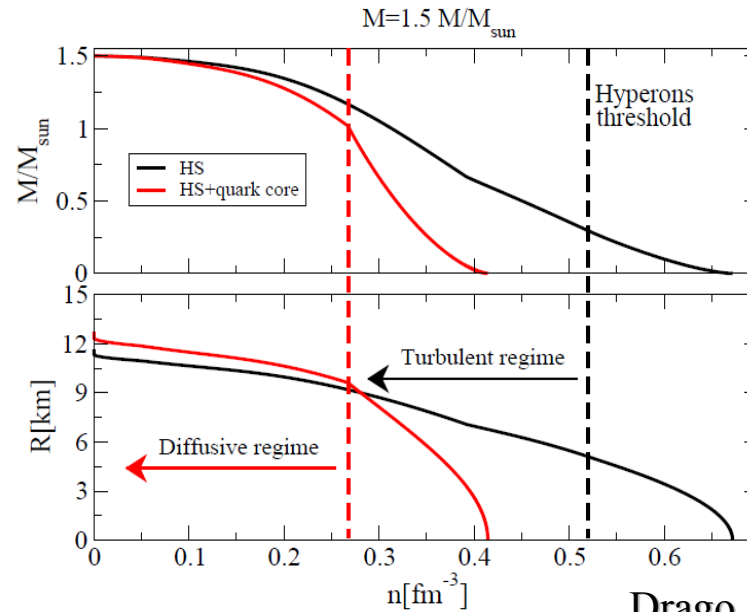
The two phases are in mechanical equilibrium. Also energy density and baryon density are continuous across the interface. But: gradient of temperature and of chemical potential. Temperature of the order of few tens MeV in the inner part of the star. Diffusion of heat/chemical species and chemical reactions allow the conversion process to proceed.



Note: the energy released during the fast conversion (time scales of ms) is emitted by the star on a much longer time scales (order of seconds) through neutrinos. Turbulent conversion and neutrino cooling are decoupled.

Modeling the diffusive regime

During the turbulent conversion both the gravitational mass and the baryonic mass are conserved (no release of neutrinos)



Drago & Pagliara 2015

FIG. 3: Enclosed gravitational mass and radius as a function of the baryon density for a $1.5M_{\odot}$ hadronic star before the turbulent conversion (black lines) and after the turbulent conversion (red lines). The black dashed line marks the appearance of hyperons: the seed of strange quark matter is formed at densities larger than this threshold. The red dashed line marks the density below which Coll's condition is no more fulfilled and the turbulent combustion does not occur anymore. Below this density, the combustion proceeds via the slow diffusive regime.

Profile of a $1.5 M_{\text{sun}}$ hadronic star and a “hybrid star”: turbulent conversion can start once hyperons appear, and it will stop 3km below the surface of the star leaving $0.5 M_{\text{sun}}$ which will burn during the diffusive regime.

State of the quark fluid as the conversion proceeds: the two phases are in mechanical equilibrium. The detonation adiabat implies that the enthalpy per baryon is conserved if the cooling process is neglected (Ex: this can be obtained also when applying the first principle of thermodynamics for a transformation at constant pressure and which conserves the total number of baryon).

$$w_A/n_A(p_A, T_A) = w_B/n_B(p_A, T_B)$$

By indicating with N the total number of baryon composing the system, the total enthalpy (for uniform matter) reads:

$$N w_A/n_A(p_A, T_A)$$

After the conversion and once the cooling is complete the system will reach again the same initial temperature (0 in our case). The total enthalpy is therefore: $N w_B/n_B(p_A, T_A)$

One can then define the heat/baryon released by the conversion as:

$$q = w_A/n_A(p_A, T_A) - w_B/n_B(p_A, T_A)$$

Does the conversion proceed until the surface of the star?

At the surface the pressure of the two phases vanishes and the enthalpy/baryon coincides with the energy/baryon.

$$e_A/n_A(T_A = 0, p_A = 0) = e_B/n_B(T_B > 0, p_A = 0) > e_B/n_B(T_B = 0, p_A = 0)$$



Energy/baryon in
the crust 930 MeV



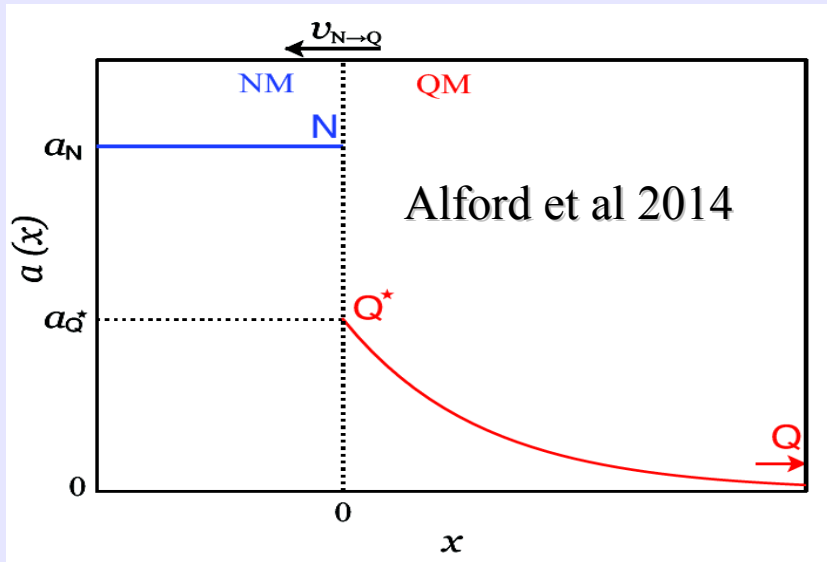
Energy/baryon of
strange quark matter
<930 MeV by hyp.

The conversion is exothermic, and thus spontaneous, until the surface. The hybrid star configurations obtained after the turbulent regime are not stable.

Propagation of the front and cooling

Within the combustion layer: diffusion and flavor changing weak interactions among quarks

$$D = 0.1 \left(\frac{\mu_q}{300 \text{ MeV}} \right)^{2/3} \left(\frac{T}{10 \text{ MeV}} \right)^{-5/3} \text{ cm}^2/\text{sec}, \quad \tau = 1.3 \times 10^{-9} \left(\frac{300 \text{ MeV}}{\mu_q} \right)^5 \text{ sec}$$



$$v_{lf} = \sqrt{\frac{D}{\tau} \frac{a_{Q*}^4}{2a_N(a_N - a_{Q*})}}$$

At fixed pressure, the minimum amount of strangeness (non-beta stable quark matter) for the process of conversion to be energetically convenient.

-) Uniform temperature, black body emission from the neutrinosphere located at r_s (we have assumed that neutrinos decouple at the inner crust-outer crust interface)

$$\frac{dr_f}{dt} = v_{lf}(\mu_q, T)$$

$$C(T) \frac{dT}{dt} = -L(T) + 4\pi r_f^2 j(r_f, T) q(r_f, T)$$

$$L = 21/8 \sigma (T/K)^4 4\pi r_s^2$$

$$C = 2 \times 10^{39} M/M_\odot (T/10^9) \text{ erg/K}$$

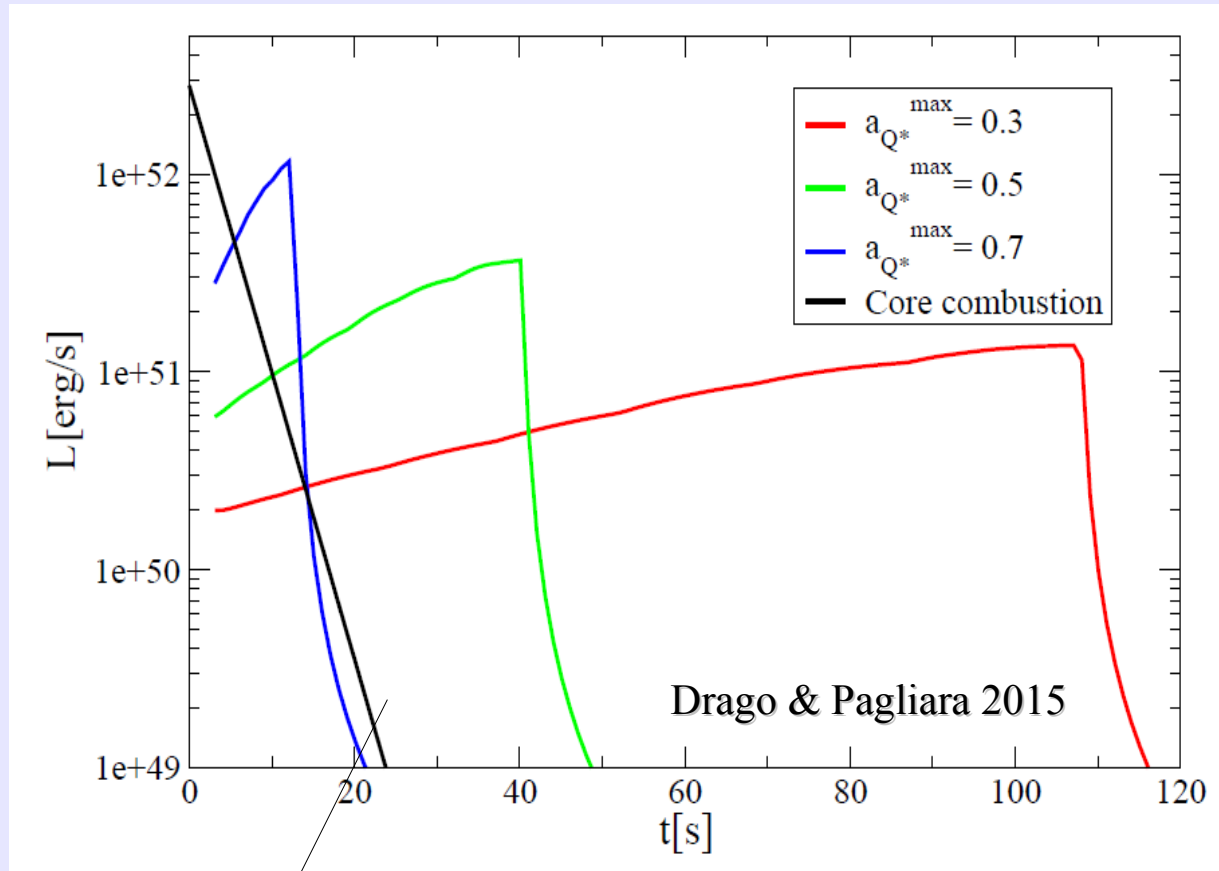


Source of heat: energy released by the conversion

$v \sim 1/T^{5/6}$ the more material is converted the higher the temperature the slower the velocity. Self-regulating mechanism!

Quasi-plateaux in the neutrino luminosity.
Unique feature of the formation of a quark star:

-) no need of a SN (the conversion could occur also for cold neutron stars)
-) if associated with a SN, this emission lasts much longer than the possible extended emission due to the fallback.

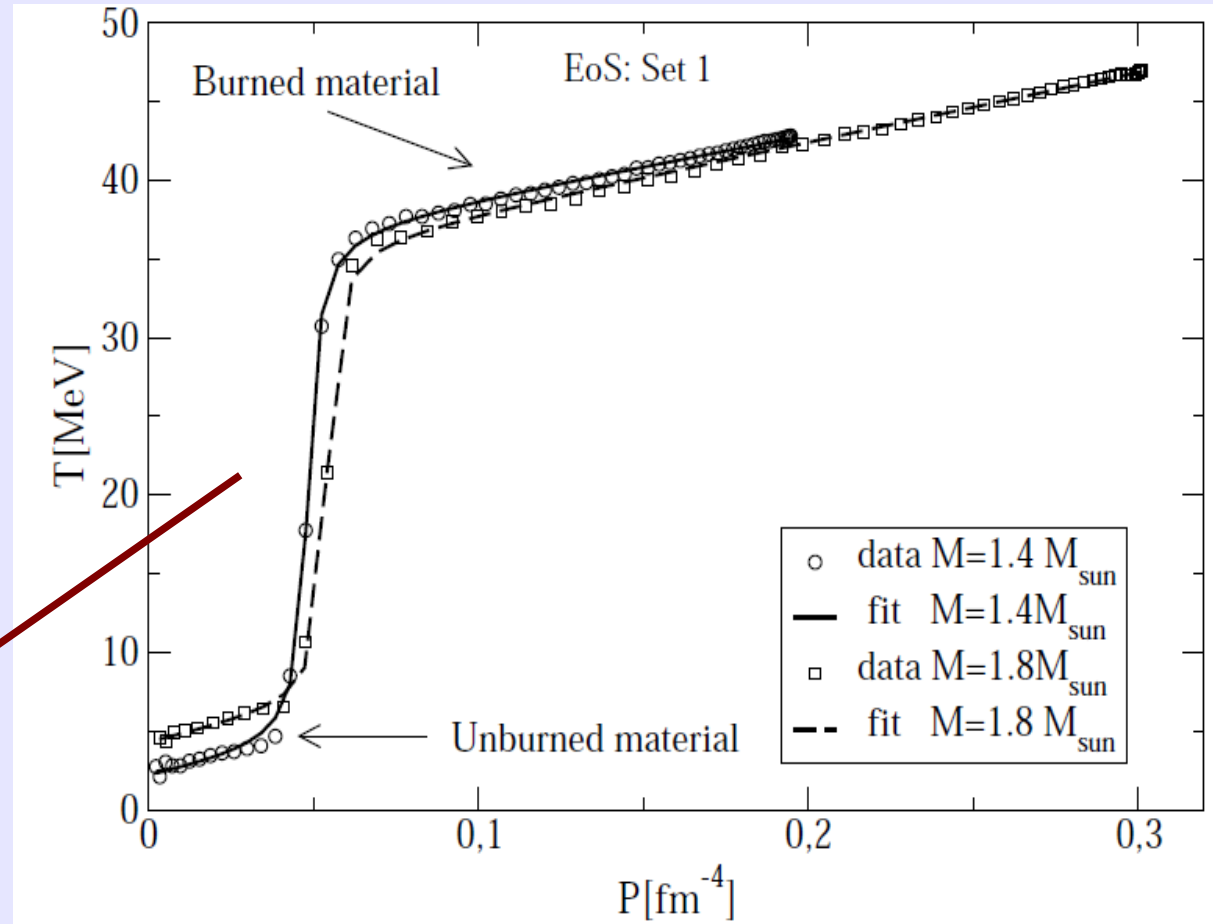


Fast decay of a standard cooling (see next slides)

Cooling of the core

The huge energy released in the burning leads to a significant heating of the star, few tens of MeV in the center.

Steep gradient of the temperature



Since the burning occurs on time scales of the order of ms, it is decoupled from the cooling (typical time scales of the order of seconds)

Temperature profiles as initial conditions for the cooling diffusion equation

Assumption: quark matter is formed already in beta equilibrium, no lepton number conservation imposed in the burning simulation, no lepton number diffusion



Diffusion is dominated by scattering of non-degenerate neutrinos off degenerate quarks

Heat transport equation due to neutrino diffusion

$$\frac{d}{dt} \frac{\epsilon_{tot}}{n_b} + P \frac{d}{dt} \frac{1}{n_b} = - \frac{\Gamma}{n_b r^2 e^\Phi} \frac{\partial}{\partial r} (e^{2\Phi} r^2 (F_{\epsilon, \nu_e} + F_{\epsilon, \nu_\mu}))$$

$$\frac{dP}{dr} = -(P + \epsilon_{tot}) \frac{m + 4\pi r^3 P}{r^2 - 2mr}$$

$$\frac{dm}{dr} = 4\pi r^2 \epsilon_{tot}$$

$$\frac{da}{dr} = \frac{4\pi r^2 n_b}{\sqrt{1 - 2m/r}}$$

$$\frac{d\Phi}{dr} = \frac{m + 4\pi r^3 P}{r^2 - 2mr}$$

$$F_{\epsilon, \nu_e} = - \frac{\lambda_{\epsilon, \nu_e}}{3} \frac{\partial \epsilon_{\nu_e}}{\partial r}$$

$$F_{\epsilon, \nu_\mu} = - \frac{\lambda_{\epsilon, \nu_\mu}}{3} \frac{\partial \epsilon_{\nu_\mu}}{\partial r}$$

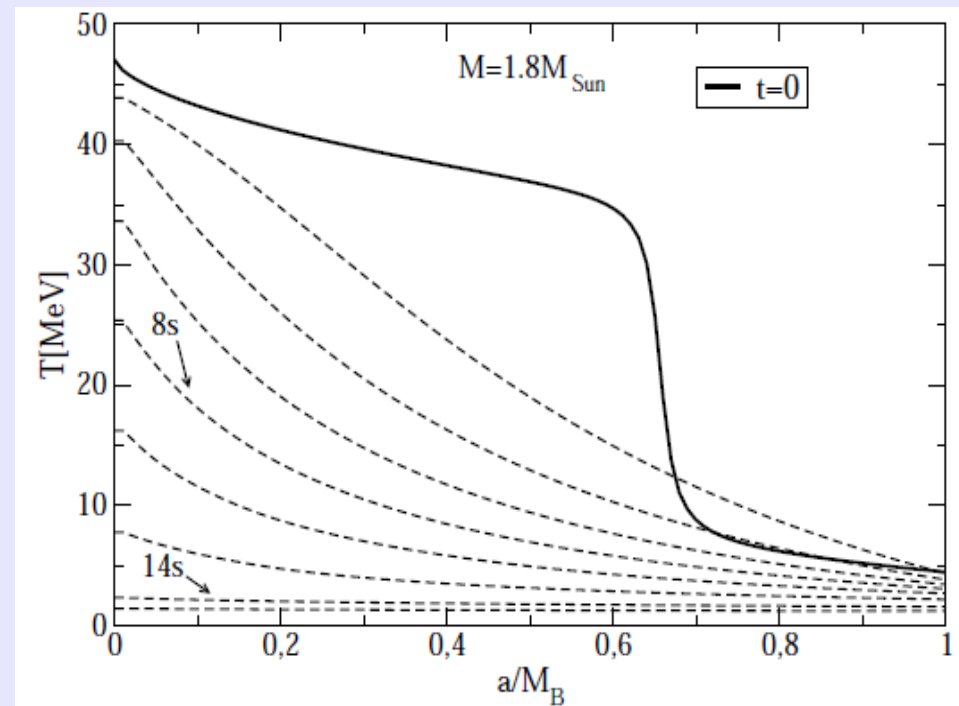
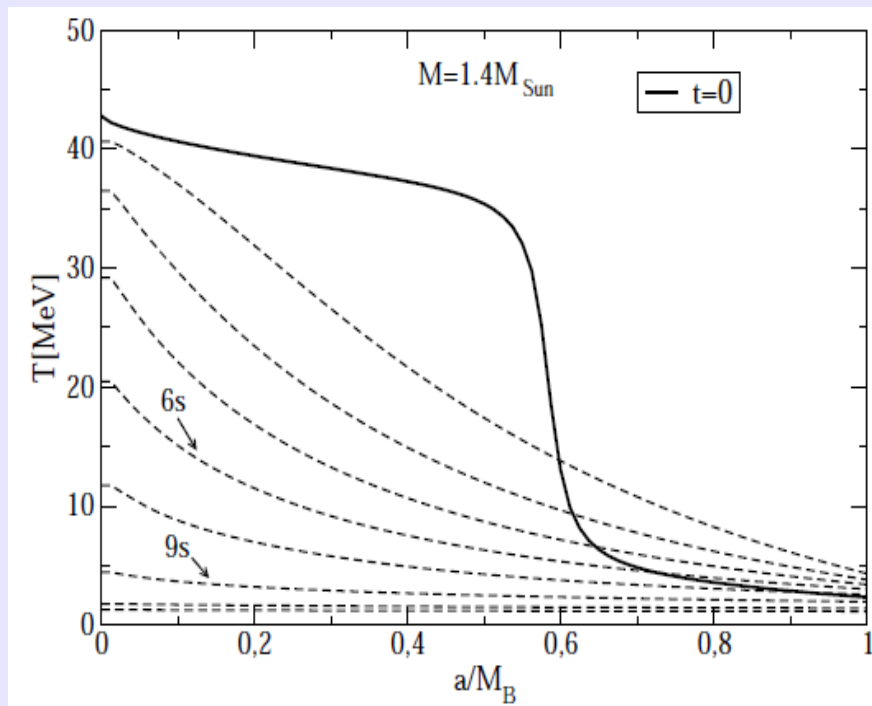
$$\frac{\sigma_S}{V} = \frac{G_F^2 E_\nu^3 \mu_i^2}{5\pi^3}$$

Steiner et al 2001

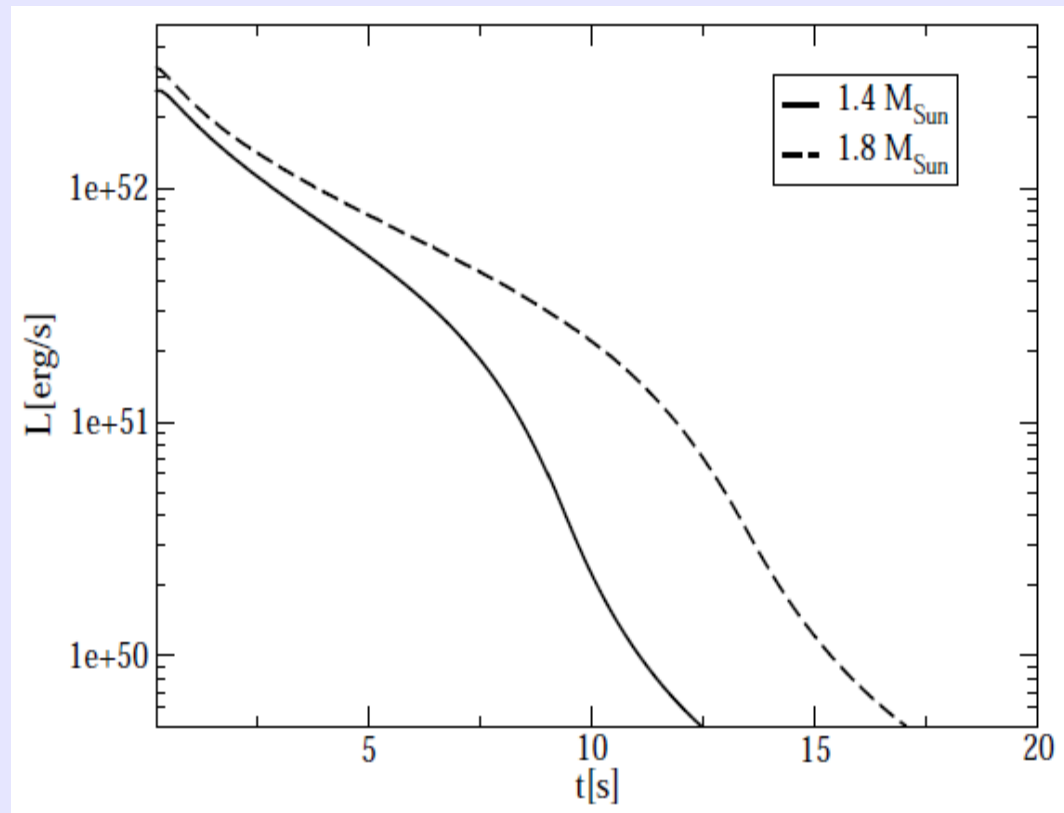
Expected smaller cooling times with respect to hot neutron stars

phase	process	$\lambda(T=5 \text{ MeV})$	$\lambda(T=30 \text{ MeV})$
Nuclear Matter	$\nu n \rightarrow \nu n$	200 m	1 cm
	$\nu_e n \rightarrow e^- p$	2 m	4 cm
Unpaired Quarks	$\nu q \rightarrow \nu q$	350 m	1.6 m
	$\nu d \rightarrow e^- u$	120 m	4 m
CFL	λ_{3B}	100 m	70 cm
	$\nu \phi \rightarrow \nu \phi$	>10 km	4 m

Reddy et al 2003



Luminosity curves similar to the protoneutron stars neutrino luminosities. Possible corrections due to lepton number conservation...



Phenomenology I: such a neutrino signal could be detected for events occurring in our galaxy (possible strong neutrino signal lacking the optical counterpart if the conversion is delayed wrt the SN)

Phenomenology II: connection with double GRBs within the protomagnetar model

UNUSUAL CENTRAL ENGINE ACTIVITY IN THE DOUBLE BURST GRB 110709B

BIN-BIN ZHANG¹, DAVID N. BURROWS¹, BING ZHANG², PETER MÉSZÁROS^{1,3}, XIANG-YU WANG^{4,5}, GIULIA STRATTA^{6,7}, VALERIO D'ELIA^{6,7}, DMITRY FREDERIKS⁸, SERGEY GOLENETSKI⁸, JAY R. CUMMINGS^{9,10}, JAY P. NORRIS¹¹, ABRAHAM D. FALCONE¹, SCOTT D. BARTHELMEY¹², NEIL GEHRELS¹²

Draft version January 17, 2012

ABSTRACT

The double burst, GRB 110709B, triggered *Swift*/BAT twice at 21:32:39 UT and 21:43:45 UT, respectively, on 9 July 2011. This is the first time we observed a GRB with two BAT triggers. In this paper, we present simultaneous *Swift* and *Konus-WIND* observations of this unusual GRB and its afterglow. If the two events originated from the same physical progenitor, their different time-dependent spectral evolution suggests they must belong to different episodes of the central engine, which may be a magnetar-to-BH accretion system.

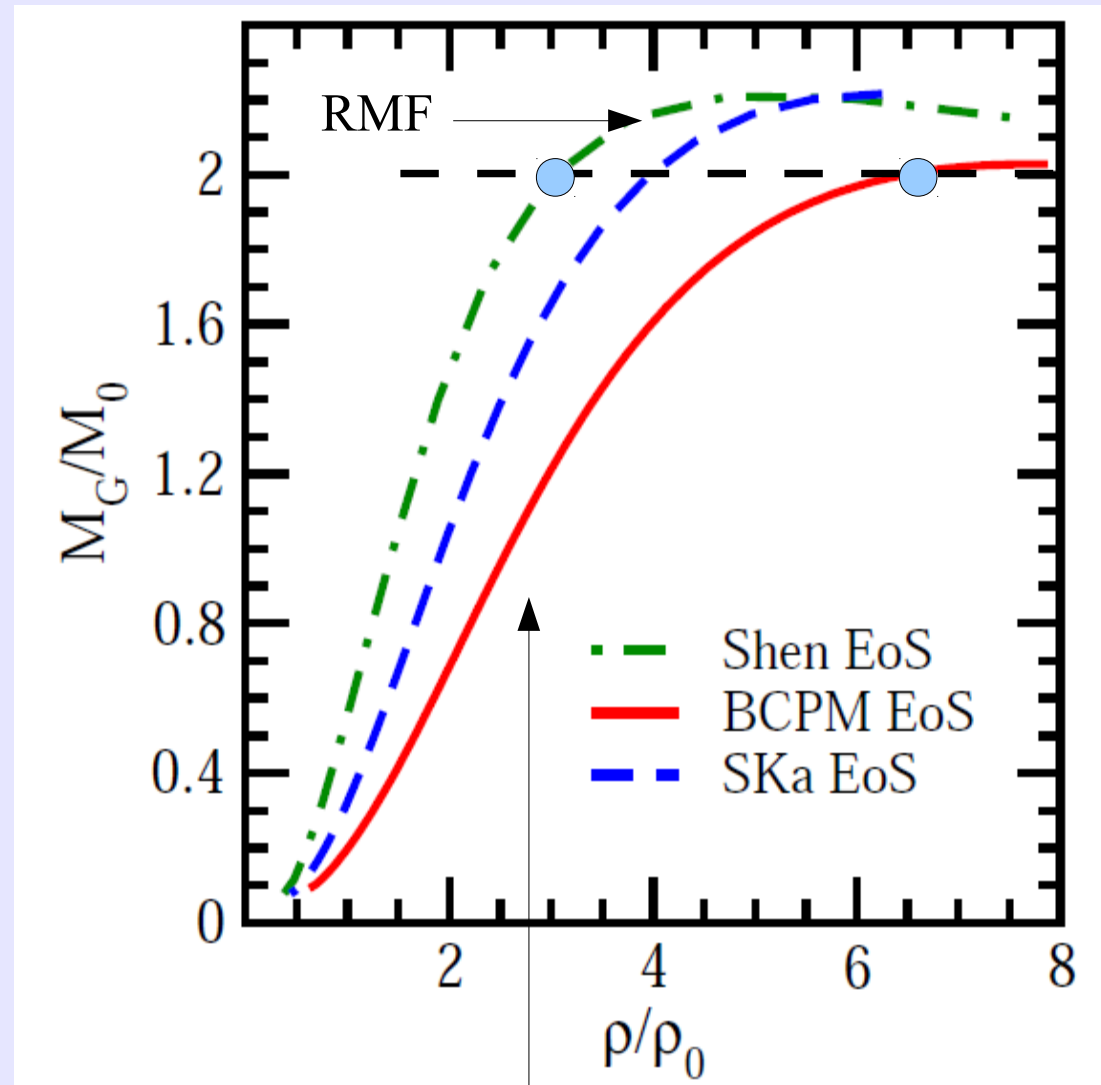
Subject headings: gamma-ray burst: general

**Why speculating about the
existence of quark stars?**

J1614-2230, what does a $2M_{\text{sun}}$ star mean?

“Standard” neutron stars, just nucleons and electrons.

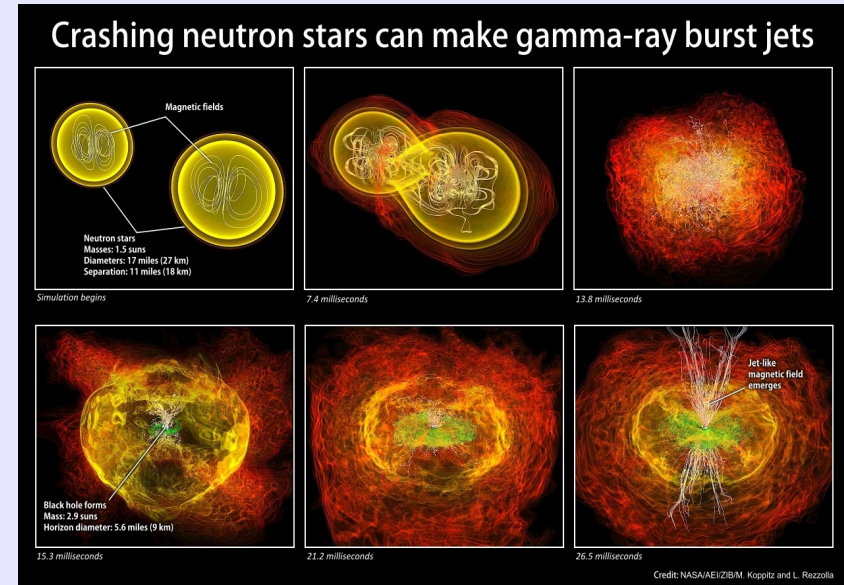
Central baryon densities of a $2M_{\text{sun}}$ star 3-7 times nuclear saturation density. Are there really just nucleons? Hyperons & Δ ?



Microscopic calculation: nucleon nucleon potential and three body forces (Baldo et al 2013)

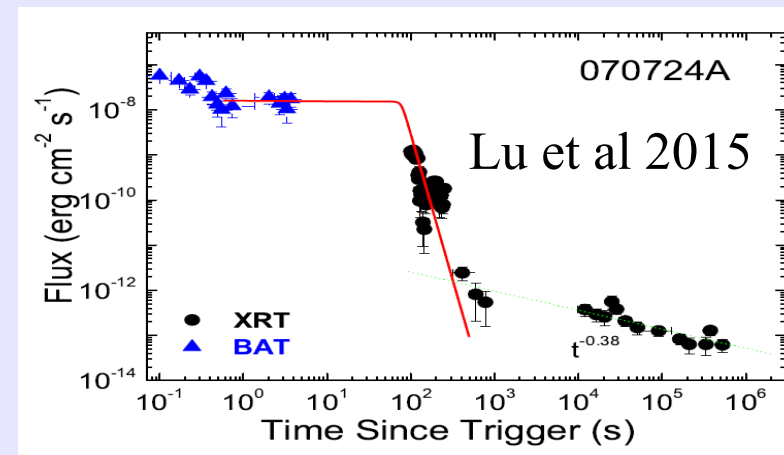
... heavier stars from shortGRB observations?

Before SWIFT: energy released 10^{51} erg, duration few hundreds of ms.
Inner engine: merger of two neutron stars with masses of about $1.3\text{--}1.5 M_{\text{sun}}$ (main motivation: no SN associated with shortGRB).



NASA/AEI/ZIB/M. Koppitz and L. Rezzolla

SWIFT has detected many shortGRB with late time activity (10^5 sec). This could imply that the remnant of the merger is a compact star and not a black hole!! **Maximum mass $\sim 2.4 M_{\text{sun}}$.**
How?



Spin down due to magnetic dipole emission:

$$P(t) = P_0 \left(1 + \frac{4\pi^2}{3c^3} \frac{B_p^2 R^6}{I P_0^2} t\right)^{1/2}$$

Relation between the maximum mass of a supramassive star and the maximum mass of the non-rotating star (it depends on the EoS)

$$M_{\text{max}} = M_{\text{TOV}} (1 + \hat{\alpha} P^{\hat{\beta}})$$

Collapse time of the supramassive star (before t_{col} the star emits the signal seen in the plateaux)

$$t_{\text{col}} = \frac{3c^3 I}{4\pi^2 B_p^2 R^6} \left[\left(\frac{M_p - M_{\text{TOV}}}{\hat{\alpha} M_{\text{TOV}}} \right)^{2/\hat{\beta}} - P_0^2 \right]$$

See talk of Zhang next week

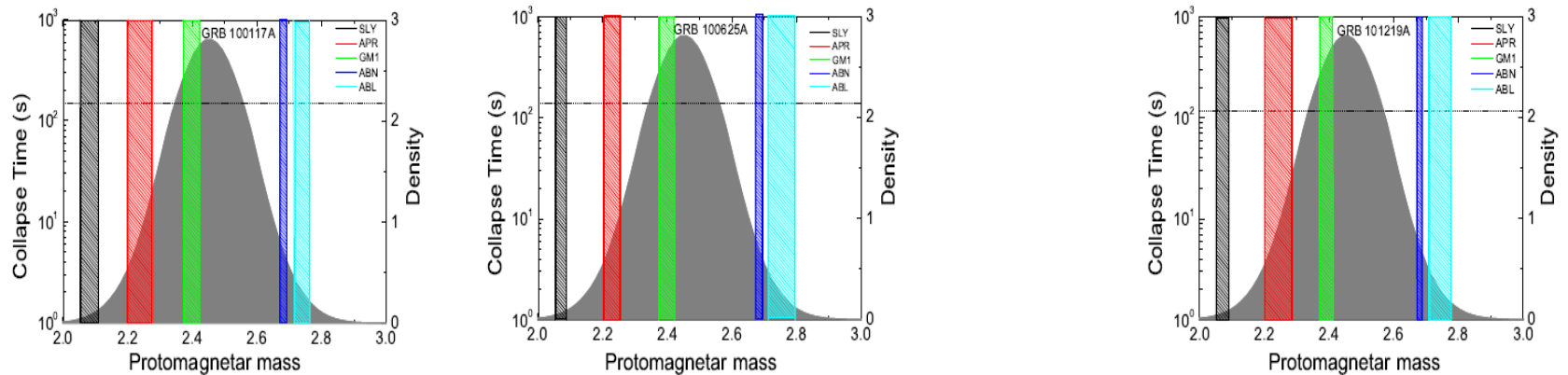
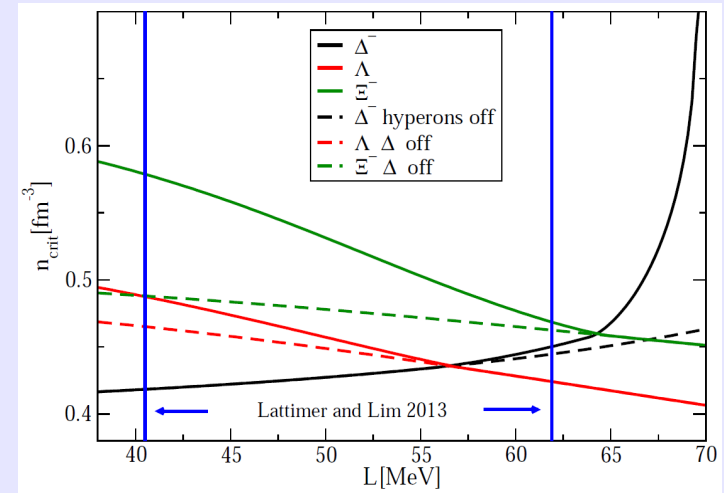
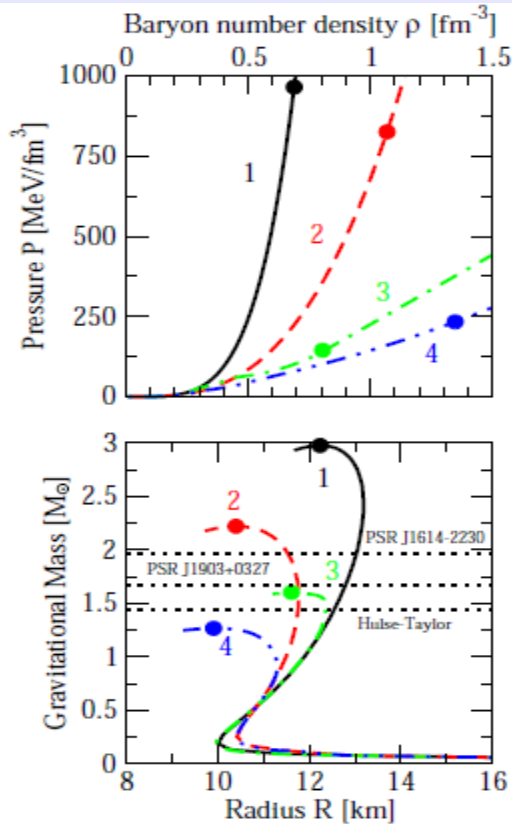


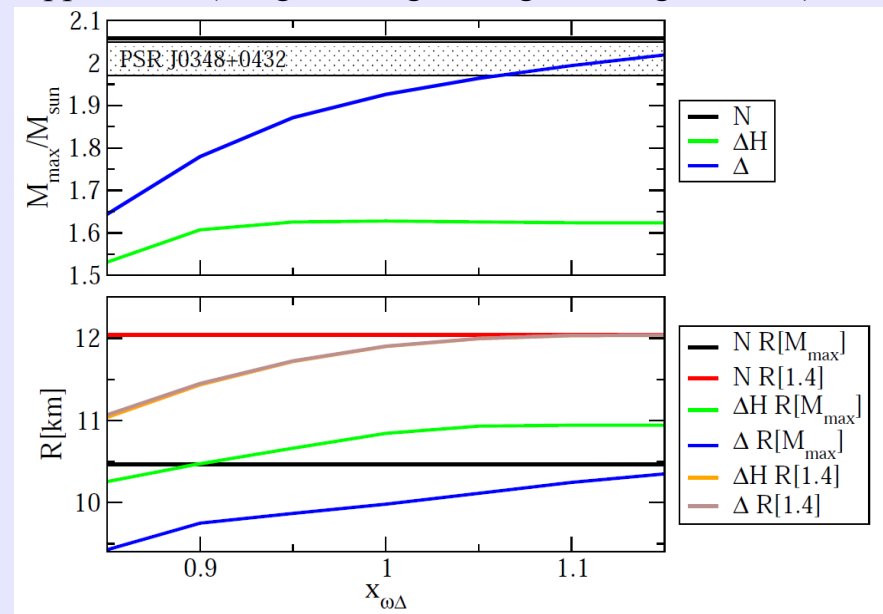
FIG. 11.— Collapse time as a function of the protomagnetar mass. The shaded region is the protomagnetar mass distribution derived from the total mass distribution of the Galactic NS–NS binary systems. The predicted results for 5 equations of state are shown in each panel: SLy (black), APR (red), GM1 (green), AB-N (blue), and AB-L (cyan). The horizontal dotted line is the observed collapse time for each GRB.

Hyperons puzzle, Δ puzzle...

Vidana et al 2011



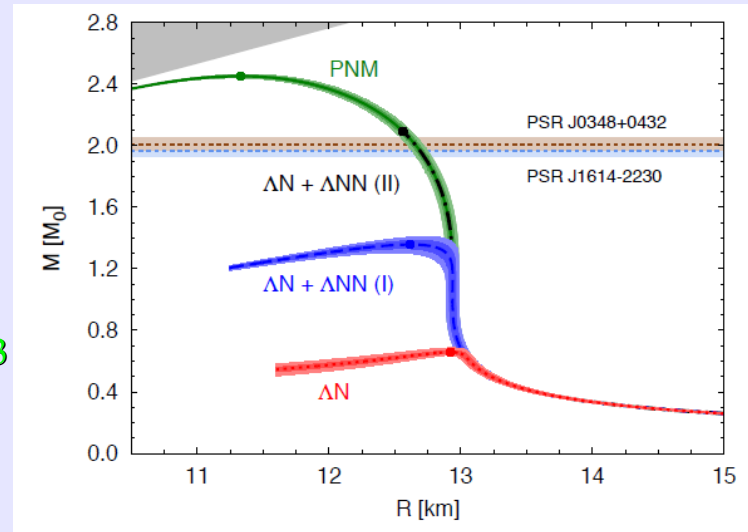
Order of 10% of reduction of the maximum mass due to Δ appearance (Drago, Lavagno, Pagliara, Pigato 2014)



Possible solutions?

Quantum MonteCarlo
simulations
(Lonardonì PRL 2015)

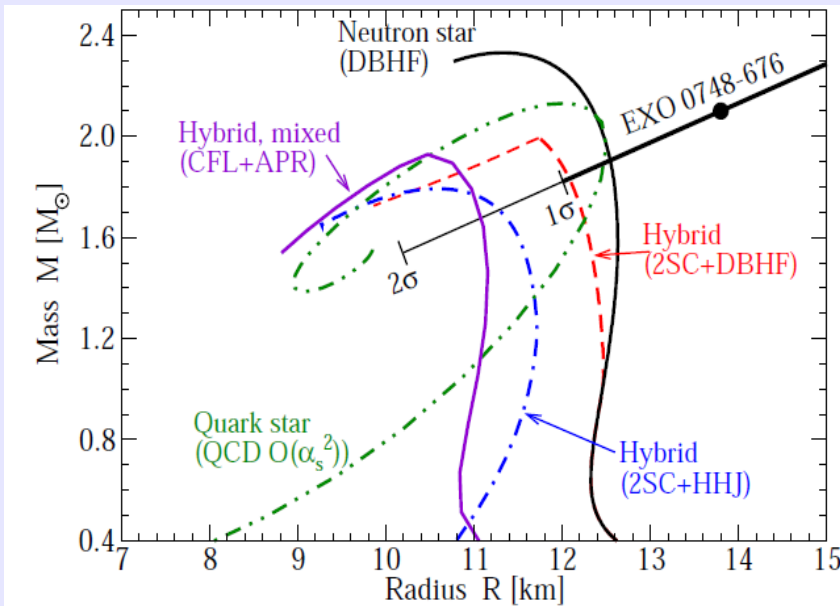
A strong $NN\Lambda$
repulsion prevents the
appearance of Λ for
densities up to $\sim 0.6\text{fm}^{-3}$



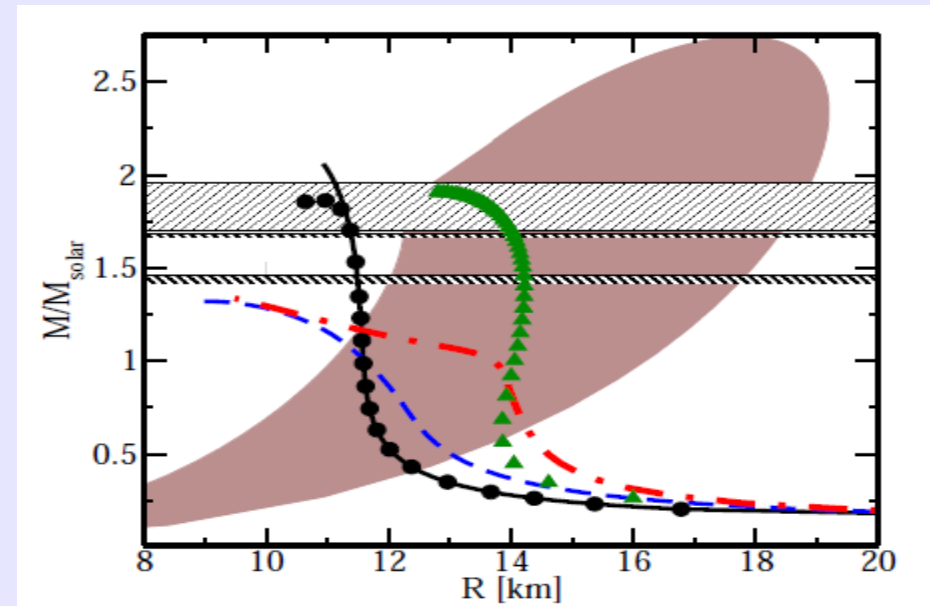
Multi-pomeron exchange potentials (see talks of Rijken and Yamamoto)

Density dependent meson masses (see talk of Kolomeitsev)

Stars containing quark matter?



Alford et al Nature 2006



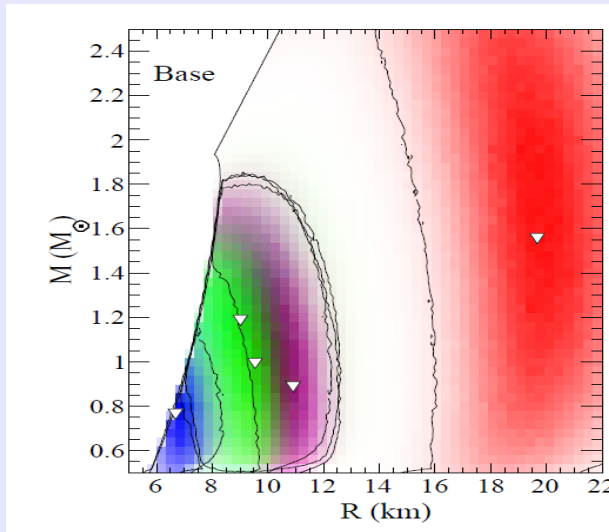
Kurkela et al 2010

pQCD calculations: “ ... equations of state including quark matter lead to hybrid star masses up to $2M_\odot$, in agreement with current observations. For strange stars, we find maximal masses of $2.75M_\odot$ and conclude that confirmed observations of compact stars with $M > 2M_\odot$ would strongly favor the existence of stable strange quark matter”

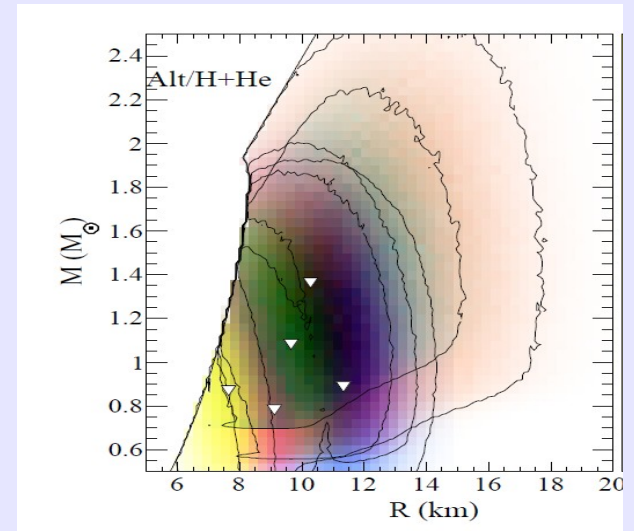
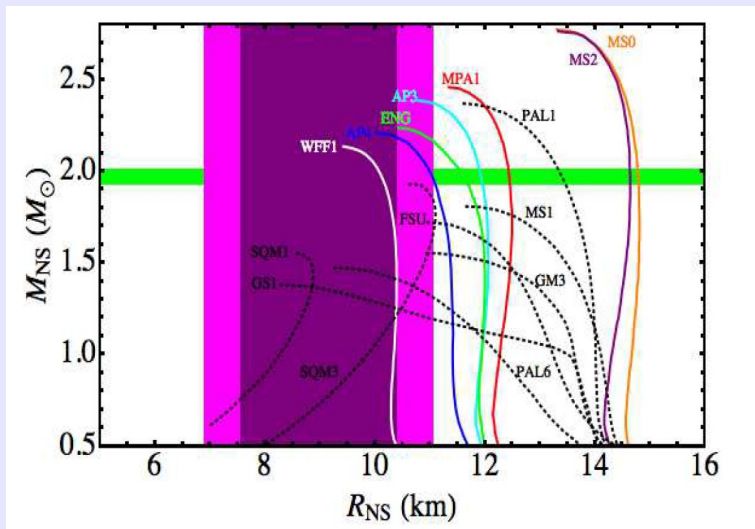
Before the discoveries of the two $2M_{\text{sun}}$ stars!!

Measurements of small radii?

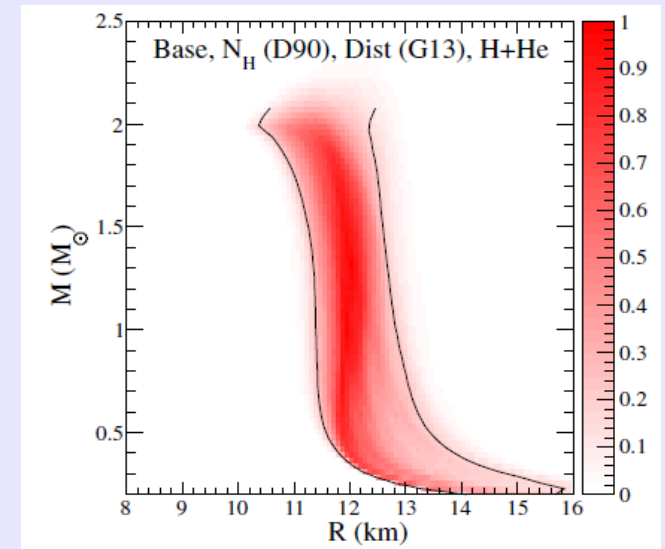
see talk of J. Lattimer next week

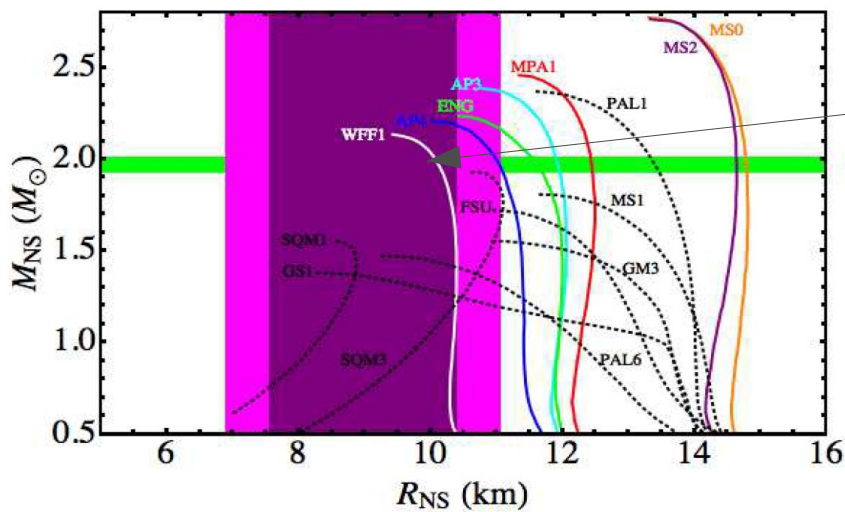


Guillot et al. ApJ (2013)

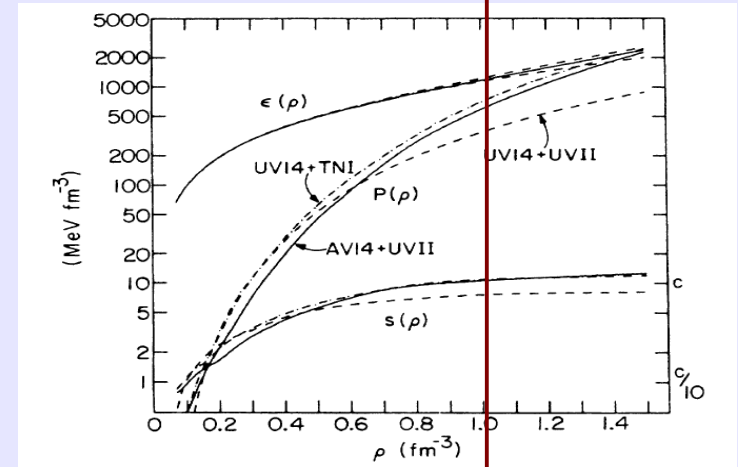


Lattimer and Steiner APJ (2014)





Wiringa et al 1988, nice, but:



It violates causality

the canonical $1.4 M_{\odot}$ neutron star has a central density $\rho_c = 0.57 \text{ fm}^{-3}$ for UV14 plus UVII and 0.66 fm^{-3} for both AV14 plus UVII and UV14 plus TNI, where the

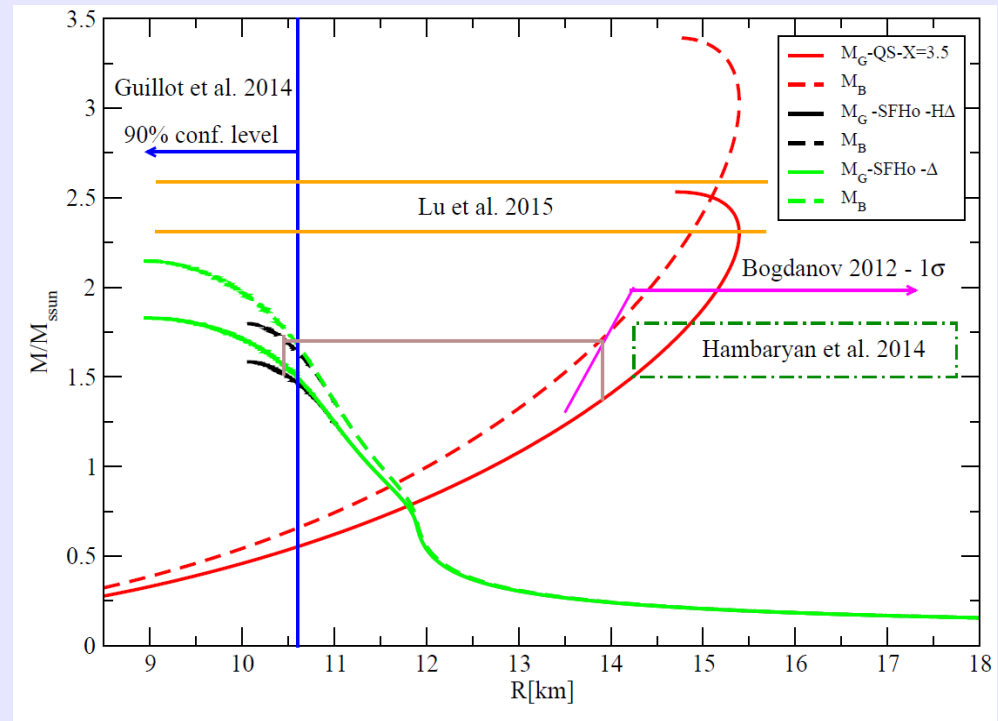
Only nucleons up to very large densities.
Similarly for AP4

Tension between different measurements:

high masses → stiff equation of state
small radii → soft equation of state
→ large central densities
→ formation of new particles

Two families of compact stars:

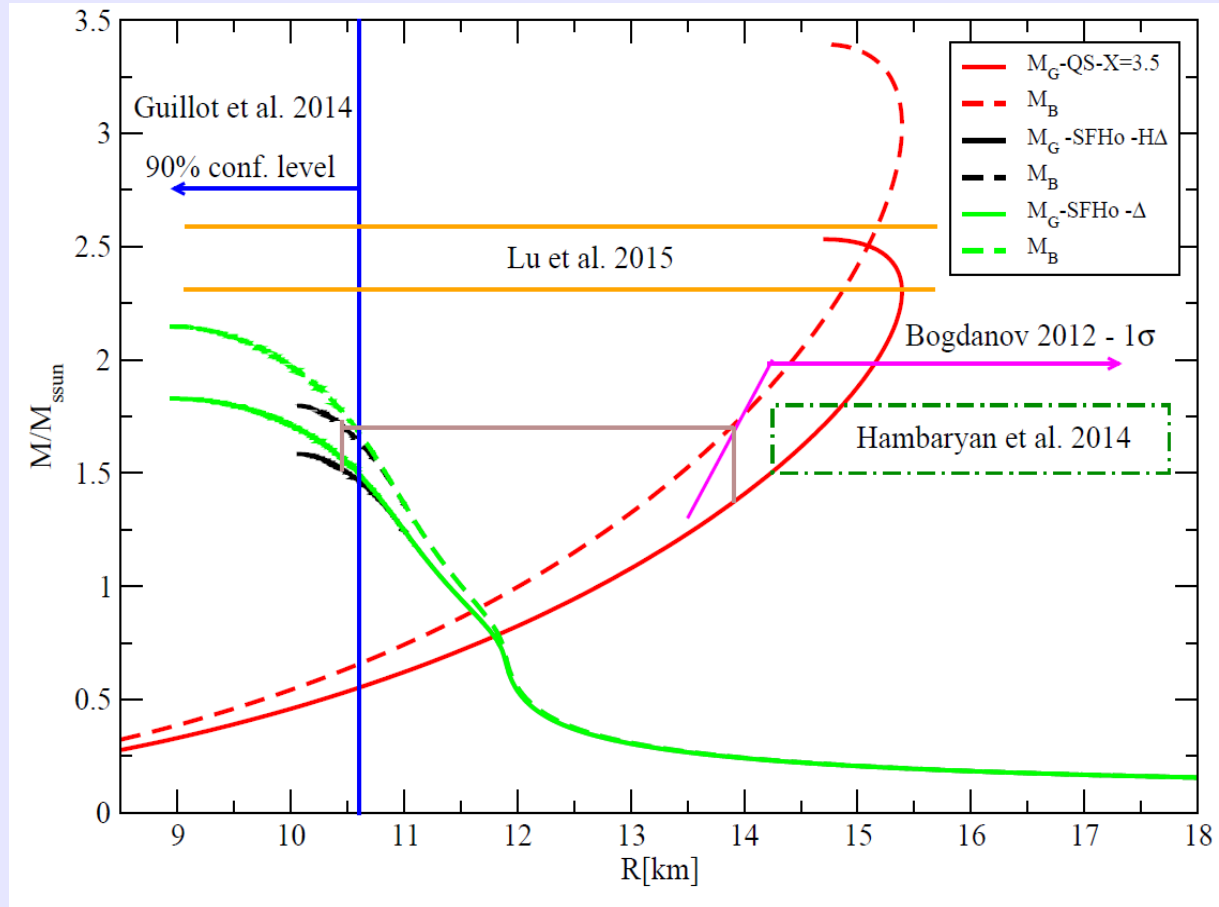
Results from RMF models for hadronic matter and simple parametrizations for the pQCD results (Fraga et al 2014)



Berezhiani et al 2003 , Drago, Lavagno, G.P. 2013 – Drago, Lavagno, G.P. , Pigato 2014-2015

- 1) low mass (up to $\sim 1.5 M_{\text{sun}}$) and small radii (down to $\sim 10 \text{ km}$) stars are hadronic stars (containing nucleons, Δ and hyperons) and they are metastable
- 2) high mass and large radii stars are strange stars (strange matter is absolutely stable (Bodmer-Witten hyp.))

**Why conversion
should then occur?
Quark stars are more
bound: at a fixed
total baryon number
they have a smaller
gravitational mass
wrt hadronic stars**



Two families and short/long GRBs

Internal X-ray plateau in short GRBs: Signature of supramassive fast-rotating quark stars?

Ang Li^{1,2*}, Bing Zhang^{2,3,4†}, Nai Bo Zhang⁵, He Gao⁶, Bin Qi⁵, Tong Liu^{1,2}

¹ Department of Astronomy, Xiamen University, Xiamen, Fujian 361005, China

² Department of Physics and Astronomy, University of Nevada Las Vegas, Nevada 89154, USA

³ Department of Astronomy, School of Physics, Peking University, Beijing 100871, China

⁴ Kavli Institute of Astronomy and Astrophysics, Peking University, Beijing 100871, China

⁵ Institute of Space Sciences, Shandong University, Weihai 264209, China

⁶ Department of Astronomy, Beijing Normal University, Beijing 100875, China

(Dated: June 10, 2016)

A supramassive, strongly-magnetized millisecond neutron star (NS) has been proposed to be the candidate central engine of at least some short gamma-ray bursts (SGRBs), based on the “internal plateau” commonly observed in the early X-ray afterglow. While a previous analysis shows a qualitative consistency between this suggestion and the Swift SGRB data, the distribution of observed break time t_b is much narrower than the distribution of the collapse time of supramassive NSs for the several NS equations-of-state (EoSs) investigated. In this paper, we study four recently-constructed “unified” NS EoSs (BCPM, BSk20, BSk21, Shen), as well as three developed strange quark star (QS) EoSs within the new confinement density-dependent mass (CDDM) model, labelled as CDDM, CDDM1, CDDM2. All the EoSs chosen here satisfy the recent observational constraints of the two massive pulsars whose masses are precisely measured. We construct sequences of rigidly rotating NS/QS configurations with increasing spinning frequency f , from non-rotating ($f = 0$) to the Keplerian frequency ($f = f_K$), and provide convenient analytical parametrizations of the results. Assuming that the cosmological NS-NS merger systems have the same mass distribution as the Galactic NS-NS systems, we demonstrate that all except the BCPM NS EoS can reproduce the current 22% supramassive NS/QS fraction constraint as derived from the SGRB data. We simultaneously simulate the observed quantities (the break time t_b , the break time luminosity L_b and the total energy in the electromagnetic channel E_{total}) of SGRBs, and find that while equally well reproducing other observational constraints, QS EoSs predict a much narrower t_b distribution than that of the NS EoSs, better matching the data. We therefore suggest that the post-merger product of NS-NS mergers might be fast-rotating supramassive QSs rather than NSs.

Within the proto-magnetar model of sGRBs, the formation of a quark star instead of a hadronic star in the merger would explain why the prompt phase of sGRBs is short (Drago, Lavagno, Metzger, Pagliara 2016)

Deconfinement and the protomagnetar model of long GRB

(Pili et al. 2016)

Conversion of rotating HSs

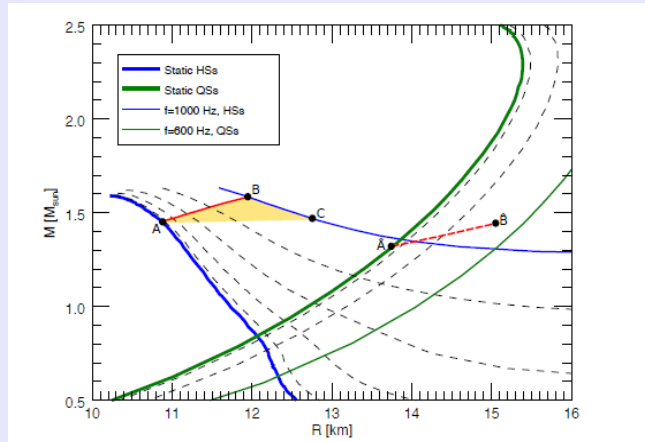


Figure 2. Gravitational mass as a function of the circumferential radius for both HSs and QSs. Thin dashed lines are sequences of stars at a fixed frequency from the non-rotating configurations (thick solid blue and green lines) to the configurations rotating at the maximum frequency (thin solid blue and green lines) and spaced by 200 Hz. The yellow region shows hadronic configurations centrifugally supported against deconfinement. Red lines and labels are the same as in figure 1.

Delayed deconfinement

Table 2. Spin-down timescales to start quark deconfinement Δt_{sd} together with the associated variation of the rotational kinetic energy ΔK_{sd} starting from an initial spin period P_i for the equilibrium sequences shown in figure 3. We also report the spin-down timescales Δt_q (defined as the time needed to half the rotational frequency of the QS) and the corresponding rotational energy loss ΔK_q after quark deconfinement. The initial magnetic field is of 10^{15} G.

M_0 [M_\odot]	$P_i \rightarrow P_d$ [ms]	Δt_{sd}	ΔK_{sd} [10^{52} erg]	Δt_q	ΔK_q [10^{52} erg]
1.666	$1.0 \rightarrow \infty$	∞	5.91	-	-
1.677	$1.0 \rightarrow 3.3$	2.7 hr	5.48	37 hr	0.19
	$2.0 \rightarrow 3.3$	1.8 hr	0.82		
	$3.0 \rightarrow 3.3$	37 min	0.13		
1.687	$1.0 \rightarrow 2.5$	1.5 hr	5.13	21 hr	0.33
	$2.0 \rightarrow 2.5$	36 min	0.46		
1.698	$1.0 \rightarrow 2.0$	55 min	4.68	14 hr	0.53
1.733	$1.0 \rightarrow 1.4$	23 min	3.37	8.2 hr	1.20
1.785	$1.0 \rightarrow 1.1$	6 min	1.37	5.4 hr	1.95
1.820	$1.0 \rightarrow 1.0$	0	0	4.6 hr	2.41

UNUSUAL CENTRAL ENGINE ACTIVITY IN THE DOUBLE BURST GRB 110709B

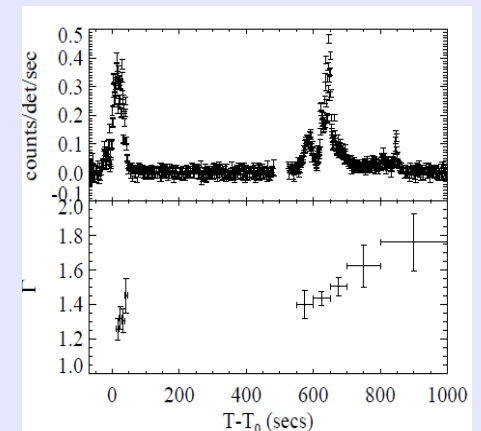
BIN-BIN ZHANG¹, DAVID N. BURROWS¹, BING ZHANG², PETER MÉSZÁROS^{1,3}, XIANG-YU WANG^{4,5}, GIULIA STRATTA^{6,7}, VALERIO D'ELIA^{6,7}, DMITRY FREDERIKS⁸, SERGEY GOLENETSKI⁸, JAY R. CUMMINGS^{9,10}, JAY P. NORRIS¹¹, ABRAHAM D. FALCONE¹, SCOTT D. BARTHELME¹², NEIL GEHRELS¹²

Draft version June 24, 2013

ABSTRACT

The double burst, GRB 110709B, triggered *Swift*/BAT twice at 21:32:39 UT and 21:43:45 UT, respectively, on 9 July 2011. This is the first time we observed a GRB with two BAT triggers. In this paper, we present simultaneous *Swift* and *Konus-WIND* observations of this unusual GRB and its afterglow. If the two events originated from the same physical progenitor, their different time-dependent spectral evolution suggests they must belong to different episodes of the central engine, which may be a magnetar-to-BH accretion system.

Subject headings: gamma-ray burst: general



Many examples of
“double bursts” in
the LGRBs data

Witten hypothesis: role of chiral symmetry breaking and confinement

SU(3) Quark-Meson Lagrangian

• Scalar meson sector

$$\mathcal{L}_{\text{sym.}} = \text{Tr}[(\partial^\mu M)^\dagger (\partial_\mu M)] - m_0^2 \text{Tr}(M^\dagger M) - \lambda_1 [\text{Tr}(M^\dagger M)]^2 - \lambda_2 \text{Tr}(M^\dagger M)^2.$$

$$\mathcal{L}_{\text{UIA}} = c(\det M + \det M^\dagger) \quad \mathcal{L}_{\text{ESB}} = \text{Tr}[H(M + M^\dagger)],$$

$$H = \text{diag}[h_u, h_d, h_s]$$

Zacchi et al 2015

• Vector meson sector

$$\mathcal{L}_{\text{vector}} = -\frac{1}{2} \text{Tr}[V_{\mu\nu} V^{\mu\nu}] - \frac{1}{2} \text{Tr}[A_{\mu\nu} A^{\mu\nu}] + \frac{1}{2} m_v^2 \text{Tr}[V_\mu V^\mu] + \frac{1}{2} m_a^2 \text{Tr}[A_\mu A^\mu] \quad V^{\mu\nu} = \partial^\mu V^\nu - \partial^\nu V^\mu$$

$$A^{\mu\nu} = \partial^\mu A^\nu - \partial^\nu A^\mu$$

• Quark sector

$$\mathcal{L}_{\text{quarks}} = \bar{q} i \gamma^\mu \partial_\mu q$$

$$\mathcal{L}_{q\sigma} = -g_\sigma \bar{q} (S - i \gamma^5 P) q$$

$$\mathcal{L}_{q\omega} = -g_\omega \bar{q} (V_\mu + \gamma^5 A_\mu) \gamma^\mu q$$

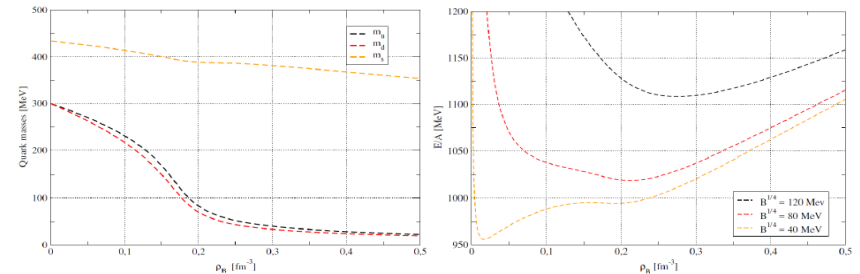
Where S,P are respectively the scalar and pseudoscalar part of the total meson matrix M

$$M = S + iP$$

Bag-like Confinement

$$\mathcal{E} \rightarrow \mathcal{E} + B$$

Where B is a constant energy density



The free parameters of the model are chosen to be:

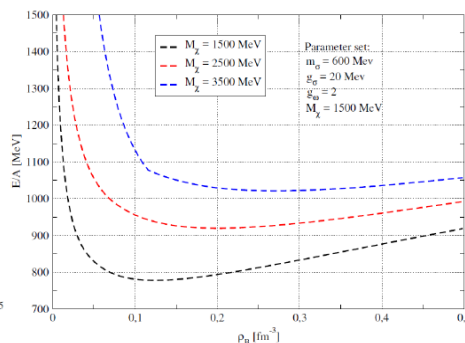
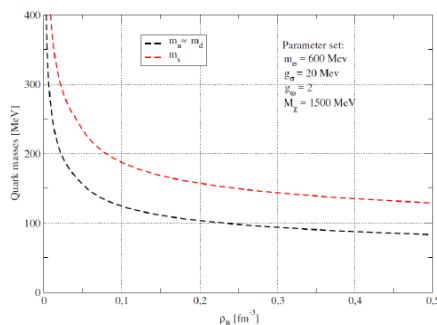
- Mass of the sigma meson $m_\sigma = 600$ MeV
- Scalar-quark coupling $g_\sigma = 300 \text{ MeV} / f_\pi$
- Vector-quark coupling $g_\omega = 2$
- The B parameter has no impact on the masses, only on the energy per baryon number.

Dielectric Confinement

$$g_\sigma \rightarrow \frac{g_\sigma}{\chi}$$

Add a whole new sector: the dielectric scalar field

$$\mathcal{L}_\chi = \frac{1}{2} (\partial_\mu \chi)^2 - \frac{1}{2} M_\chi^2 \chi^2$$



This model introduces major changes:

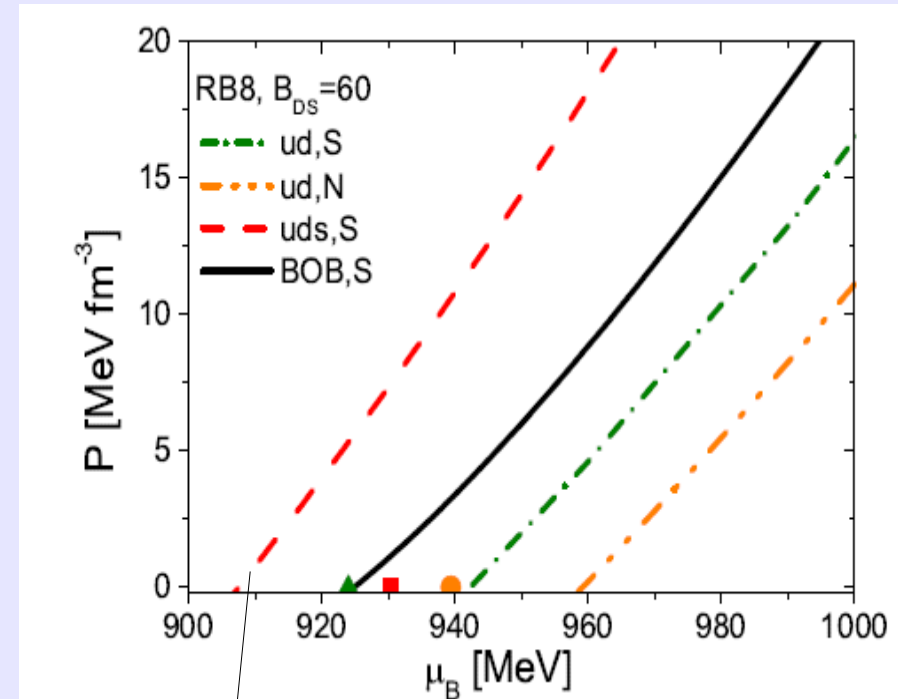
- The bag constant B is replaced with the mass of the scalar dielectric field
- The masses of the quarks are directly dependent on the confinement parameter
- This makes the quark masses decrease faster. As a result, the minimum of E/A of the system is typically lower than the bag-like case.

Preliminary results (Dondi, Drago, Pagliara in preparation): confinement is crucial for the Witten hyp. to hold true. In models featuring only chiral symmetry breaking it is hard to fulfill the Witten hyp., see Klahn & Fischer 2015

Recent findings within the
Schwinger-Dyson approach
(Chen, Wei, Schulze EPJA 2016)
Ansatz for the gluon propagator:

$$g^2(\mu)D_{\rho\sigma}(k,\mu) = 4\pi^2 d \frac{k^2}{\omega^6} e^{-\frac{k^2 + \alpha\mu^2}{\omega^2}} \left(\delta_{\rho\sigma} - \frac{k_\rho k_\sigma}{k^2} \right)$$

d and ω fitted to meson
properties, B_{DS} and α free
parameters.



In some cases stability is obtained.

Conclusions

-) New masses and radii measurements challenge nuclear physics: tension between high mass and small radii. $2.4 M_{\text{sun}}$ candidates already exist.

Possible existence of two families of compact stars (high mass – quark stars, low mass – hadronic stars). Rich phenomenology: frequency and mass distributions, explosive events, quark stars are the necessary compact remnants formed during NS mergers (if a BH is not formed promptly).

-) The conversion of a hadronic star into a quark star proceeds via two steps: turbulent regime (time scale ms) – diffusive regime (10 s)
-) Burst of neutrinos with an extended tail (important for both short and long GRB)
-) NICER, Athena+, GAIA missions, with a precision of $\sim 1\text{km}$ in radii measurements, could hopefully solve the problem.

...and **Gravitational waves!!** Smaller GW frequencies if the remnant of the merger is a quark star.

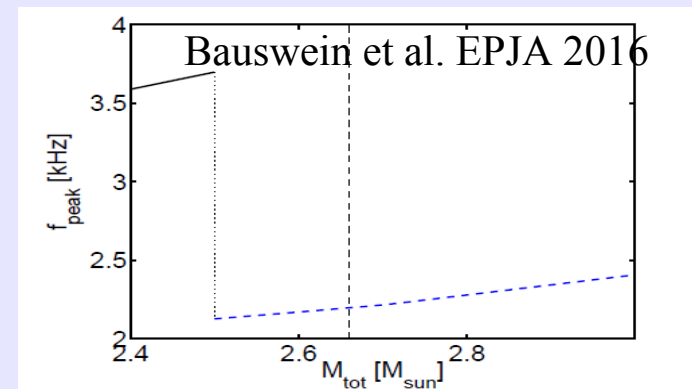
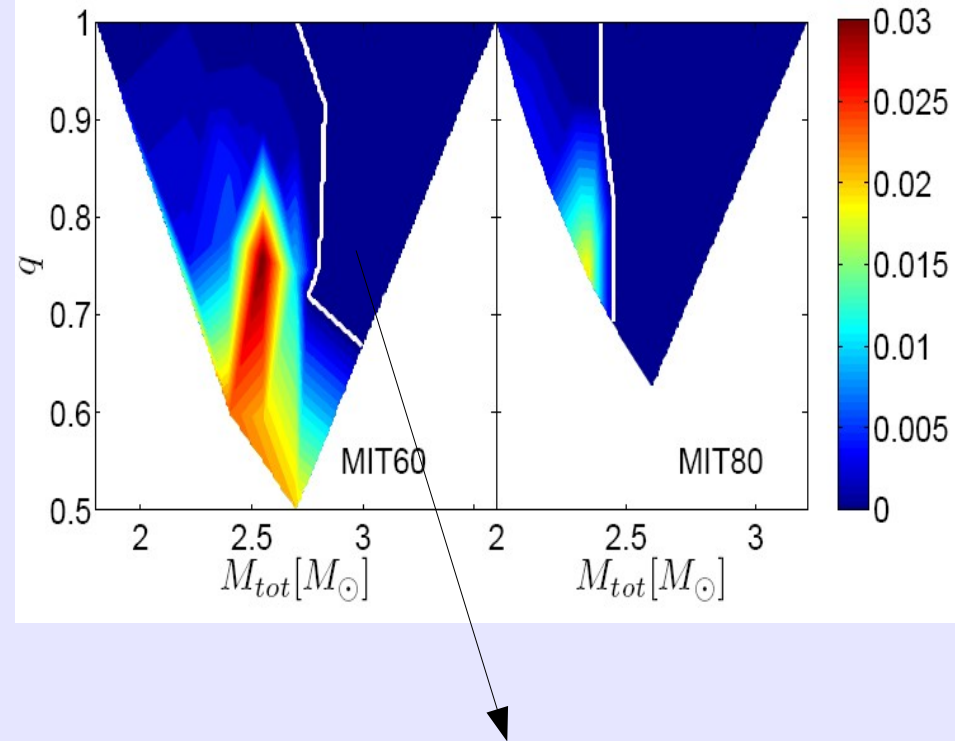
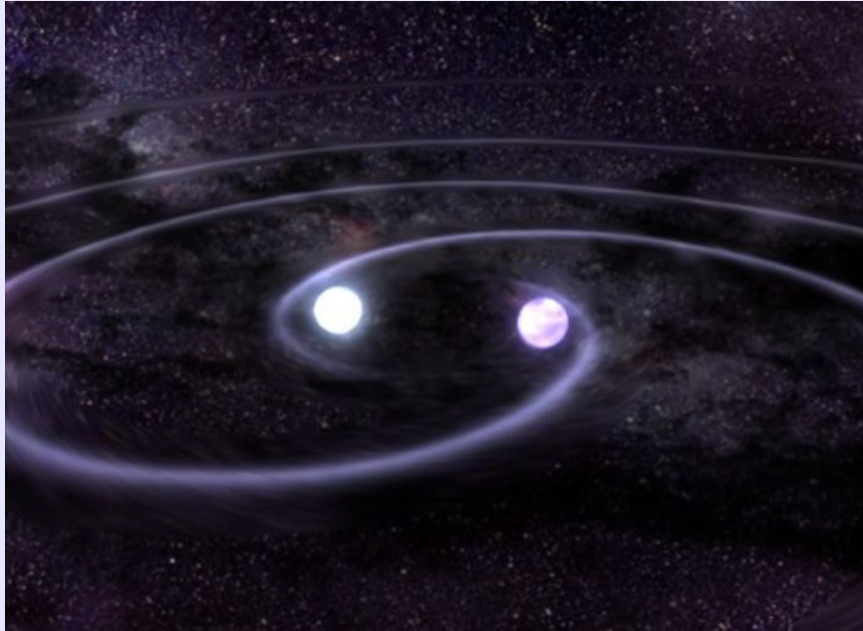


Fig. 17. Dominant postmerger GW frequency f_{peak} as a function of the total binary mass for symmetric mergers with a two-family scenario [46]. For low binary masses the merger remnant is composed of hadronic matter (black curve), whereas higher binary masses lead to the formation of a strange matter remnant with a lower peak frequency (dashed blue curve). The vertical dashed line marks a lower limit on the binary mass which is expected to yield a remnant that is stable against gravitational collapse (see text).

Appendix

Are all compact stars strange?: Merger of strange stars



MIT60: $8 \cdot 10^{-5} M_{\text{sun}}$, MIT80 no ejecta. By assuming a galactic merger rate of $10^{-4(-5)}$ /year, mass ejected: $10^{-8(-9)} M_{\text{sun}}$ /year.

Constraints on the strangelets flux (for AMS02)

A. Bauswein et al PRL (2009)

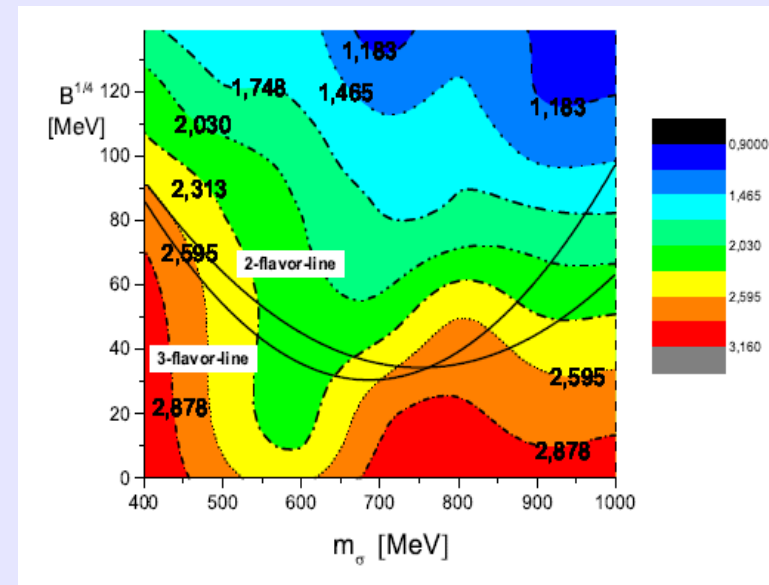
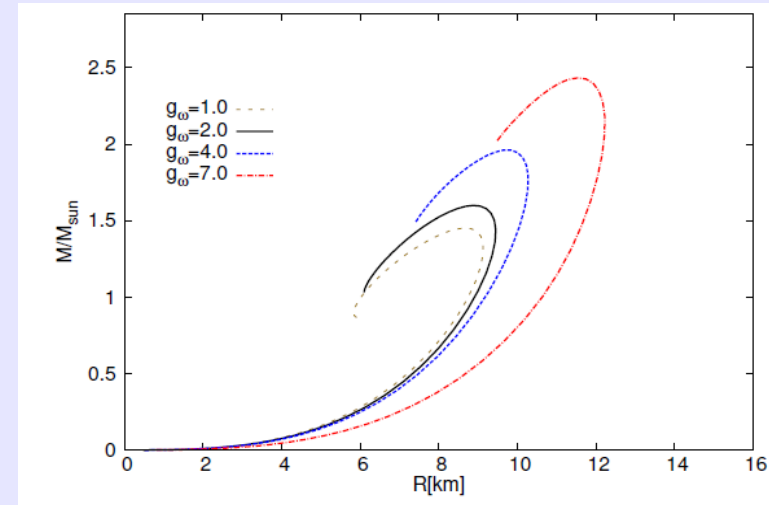
Prompt collapse: in our scenario quark stars have masses larger than $\sim 1.5 M_{\text{sun}}$, no strangelets emitted.

Quark stars within a chiral model

Mean field lagrangian

$$\begin{aligned}
 \mathcal{L} &= \mathcal{L}_M + \mathcal{L}_Q \\
 &= \frac{1}{2} (m_\omega^2 \omega^2 + m_\rho^2 \rho^2 + m_\phi^2 \phi^2) \\
 &\quad - \frac{\lambda_1}{4} (\sigma_n^2 + \sigma_s^2)^2 - \frac{\lambda_2}{4} (\sigma_n^4 + \sigma_s^4) \\
 &\quad - \frac{m_0^2}{2} (\sigma_n^2 + \sigma_s^2) + \sqrt{2} \sigma_n^2 \sigma_s c + h_n \sigma_n + h_s \sigma_s - B \\
 &\quad + \bar{\Psi}_n (i \not{\partial} - g_\omega \gamma^0 \omega - g_\rho \vec{\tau} \gamma^0 \rho - g_n \sigma_n) \Psi_n \\
 &\quad + \bar{\Psi}_s (i \not{\partial} - g_s \sigma_s - g_\phi \gamma^0 \phi) \Psi_s
 \end{aligned}$$

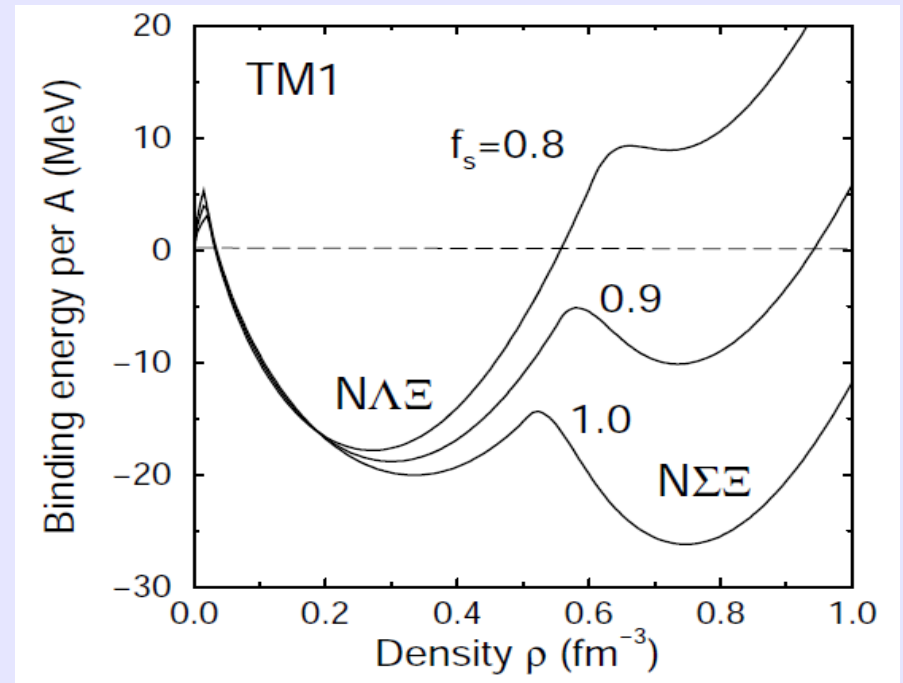
Required large mass
of the “sigma”
meson



What prevents the conversion of a metastable hadronic star?

A star containing only nucleons and Δ cannot convert into a quark star because of the lack of strangeness (need for multipole simultaneous weak interactions).

Only when hyperons start to form the conversion can take place.



New minima of BE/A could appear when increasing strangeness, (very) strange hypernuclei (Schaffner-Bielich- Gal 2000)

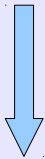
Within a simple parametrization:

$$\Omega_{QM} = \sum_{i=u,d,s,e} \Omega_i + \frac{3\mu^4}{4\pi^2}(1 - a_4) + B_{eff}$$

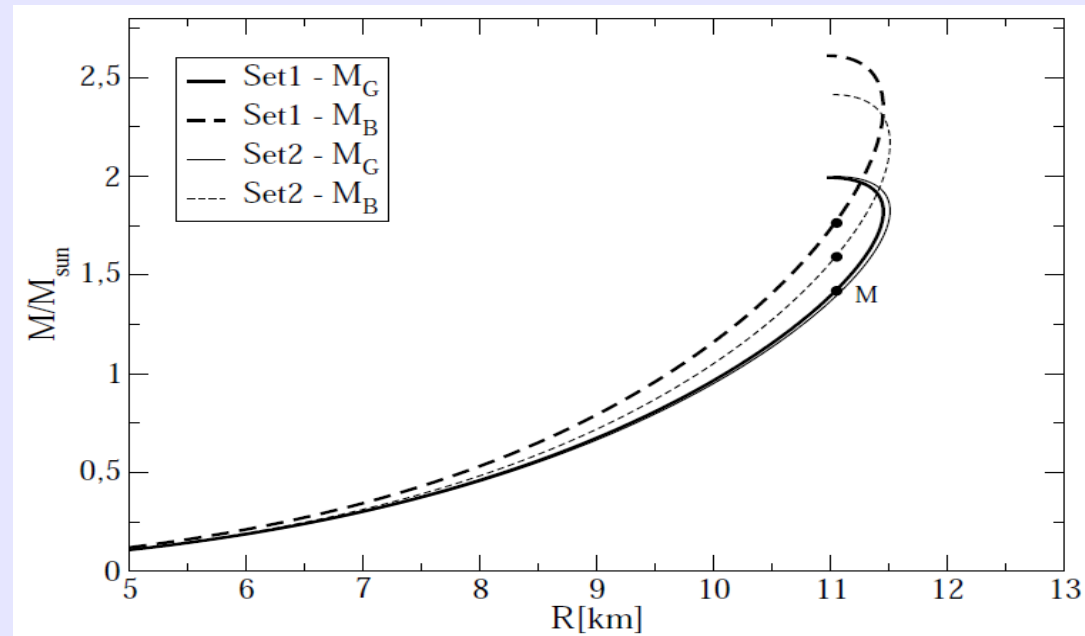
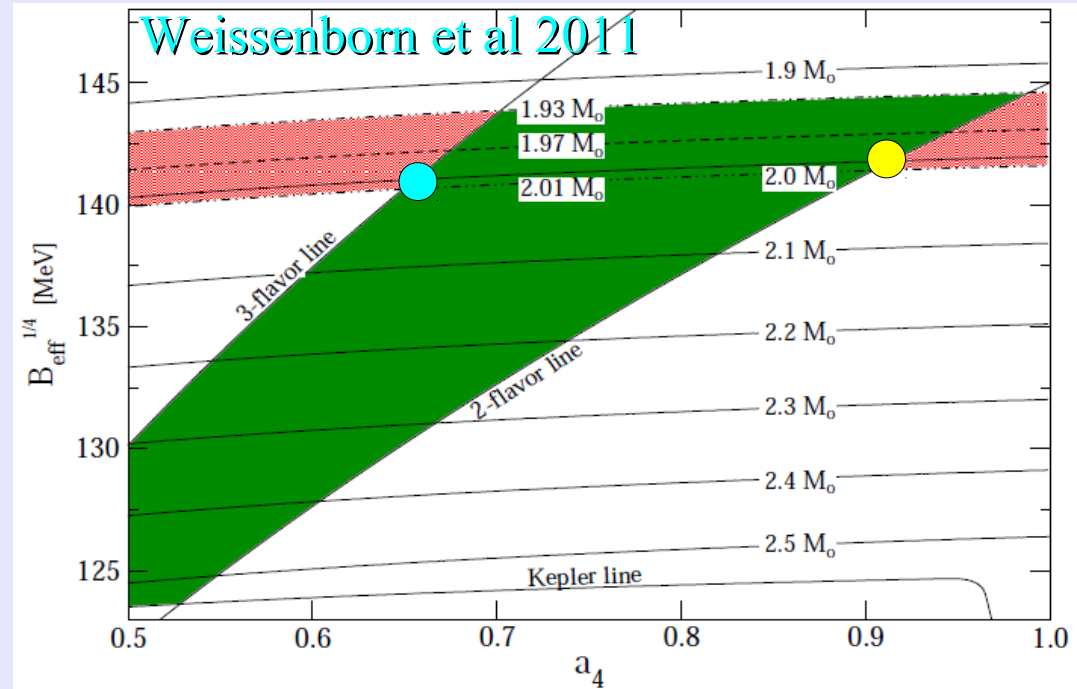
Two EoSs which provide a maximum mass of $2M_{\text{sun}}$

● $E/A=860 \text{ MeV}(\text{set1})$

● $E/A=930 \text{ MeV}(\text{set2})$



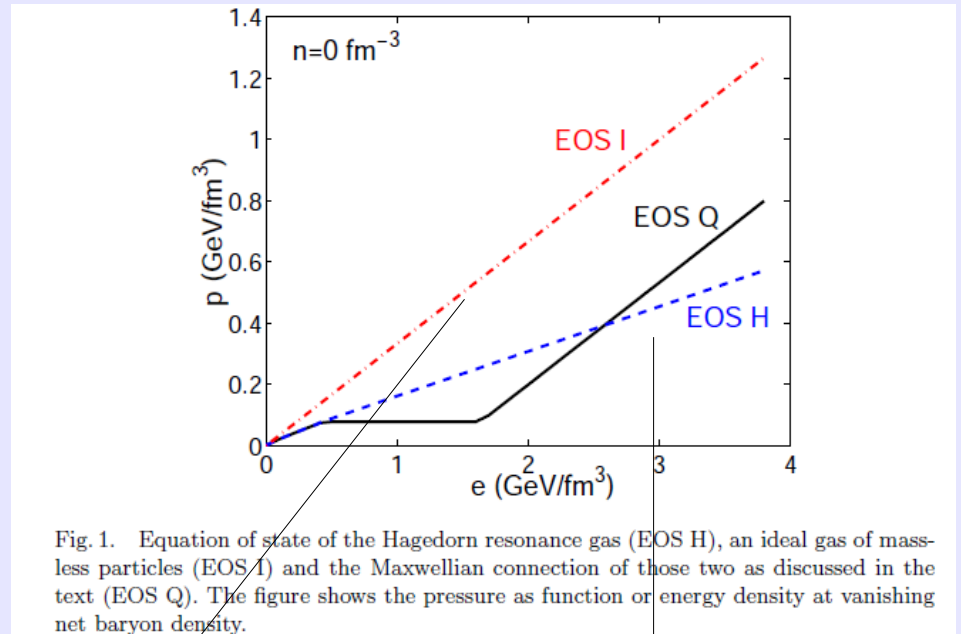
Different QSs binding energy $M_B - M_G$



... is this surprising?

Also at finite density the quark matter equation of state should be stiffer than the hadronic equation of state in which new particles are produced as the density increases

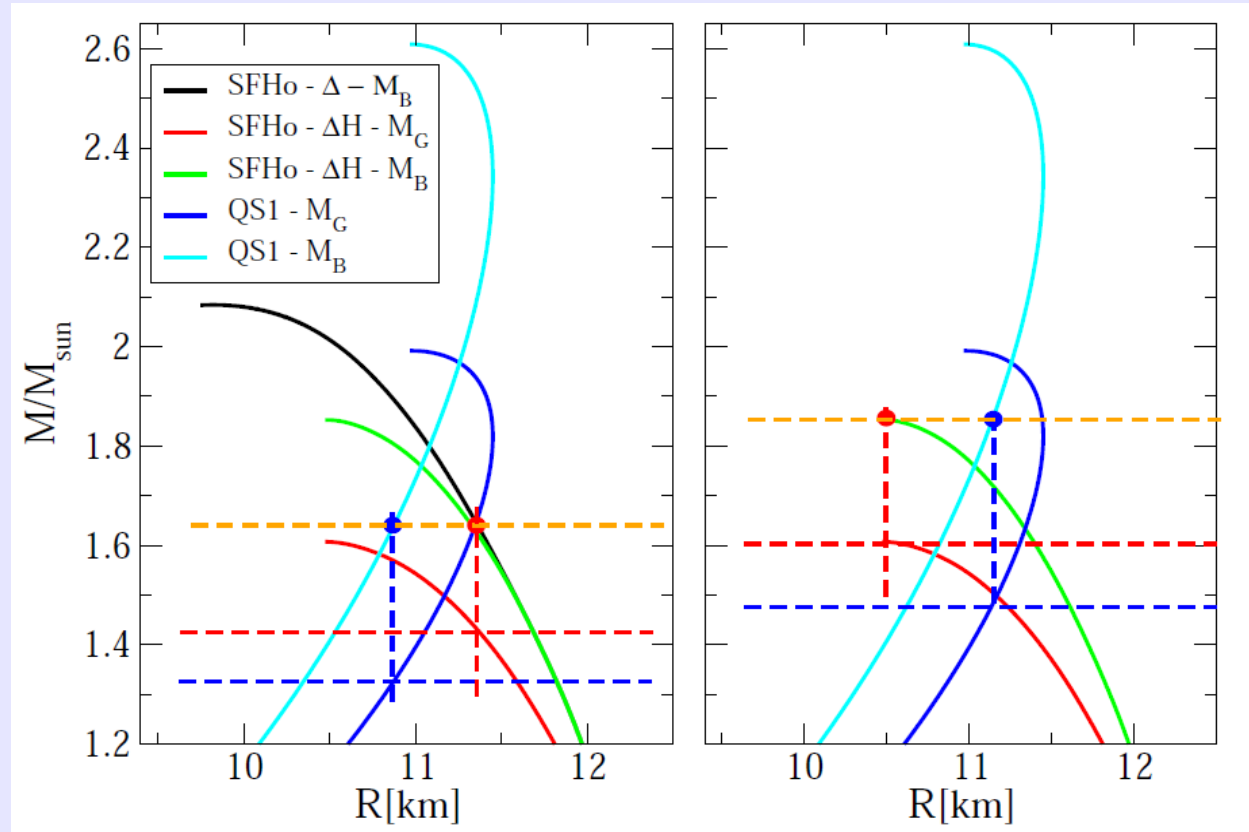
Heavy ions physics: (Kolb & Heinz 2003)



$p=e/3$ massless
quarks

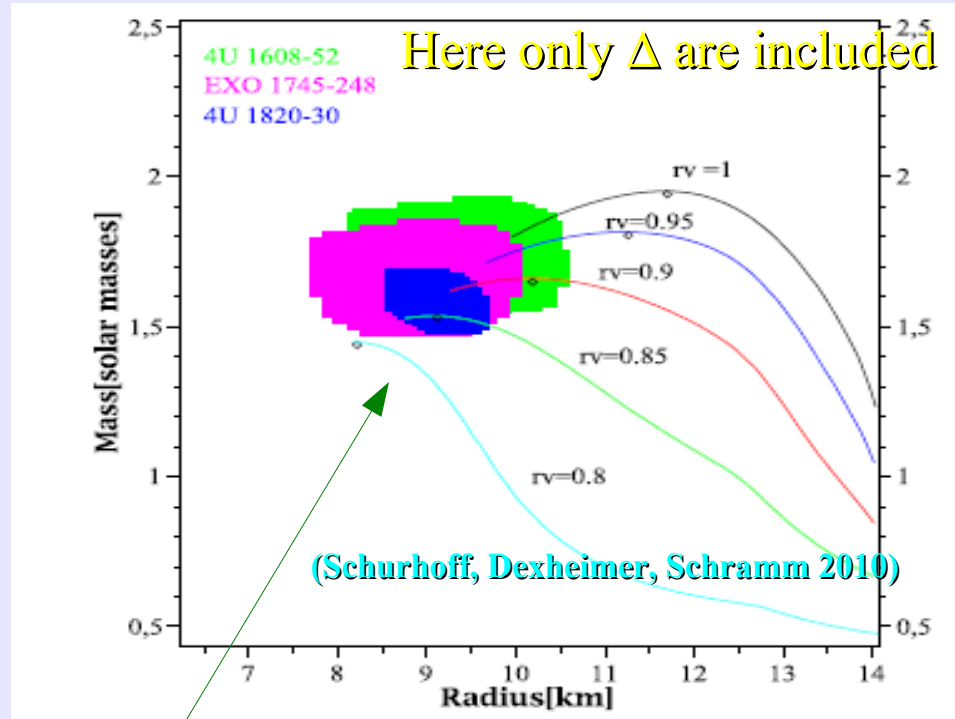
Hadron resonance gas
 $p=e/6$

**Why conversion
should then occur?
Quark stars are
more bound: at a
fixed total baryon
number they have a
smaller
gravitational mass
wrt hadronic stars**

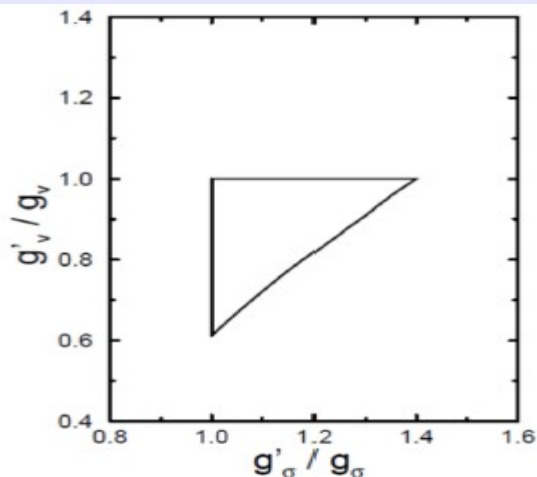


What about Δ ?

Similar effects: softening of the equation of state. Just small changes of the couplings with vector mesons sizably decrease the maximum mass



Notice: very small radii



Kosov, Fuchs, Marmyanov,
Faessler, PLB 421 (1998) 37

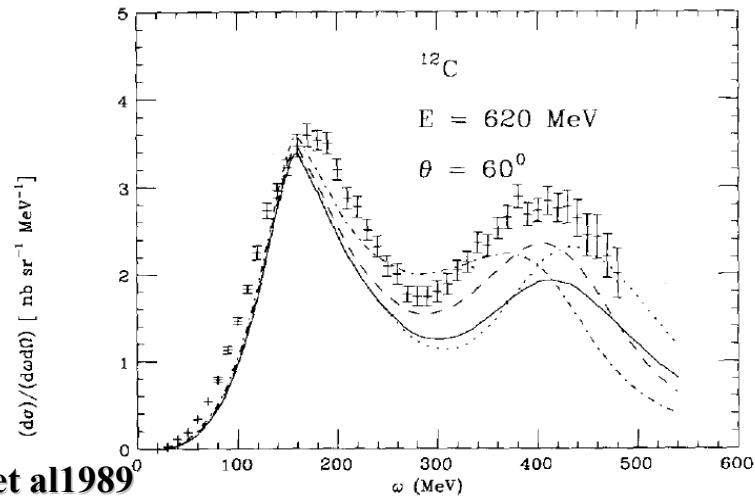
Some constraints on the couplings with mesons from nuclear matter properties and QCD sum rules

Do we have any experimental/theoretical information on $x\omega\Delta$ & $x\sigma\Delta$?

Electron, pion scattering photoabsorption on nuclei (O'Connel et al 1990, Wehrberger et al 1989...). Indications of a Δ potential in the nuclear medium deeper than the nucleon potential. Several phenomenological and theoretical analyses lead to similar conclusions.

Phenomenological potentials:

$$\begin{aligned}\omega &= E_f - E_i \\ &= (p_f^2 + W^2)^{1/2} + V_W(p_f) - (p_i^2 + M^2)^{1/2} - V_N(p_i) \\ V(p) &= -V_0 / (1 + p^2/p_0^2) + V_1\end{aligned}$$



Wehrberger et al 1989

Fig. 13. Cross section for electron scattering on ^{12}C at incident electron energy $E = 620$ MeV and scattering angle $\theta = 60^\circ$ as a function of energy transfer ω for standard nucleon and different Δ -couplings. The lines are the results for the sum of the contribution from nucleon knockout and Δ -excitation. The dotted line shows the cross section for free Δ 's, and the dashed and dot-dashed lines for no coupling to the vector field and a ratio $r_s = 0.15$ and 0.30 of the scalar coupling of the Δ to the scalar coupling of the nucleon. The solid line is obtained for universal coupling. The data are from ref. ¹⁶).

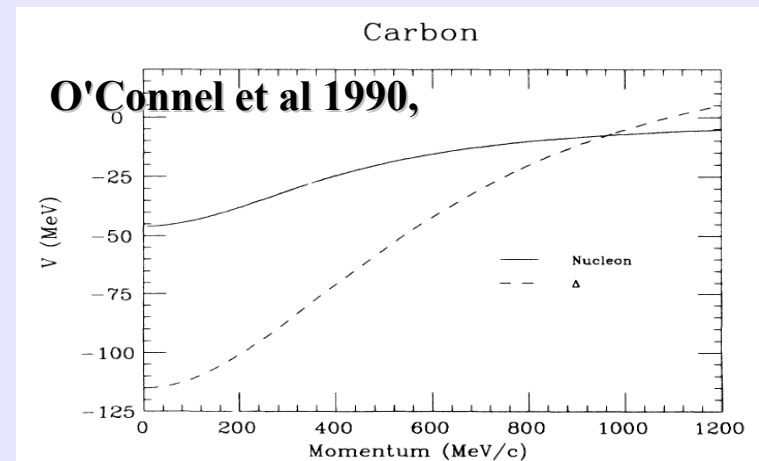
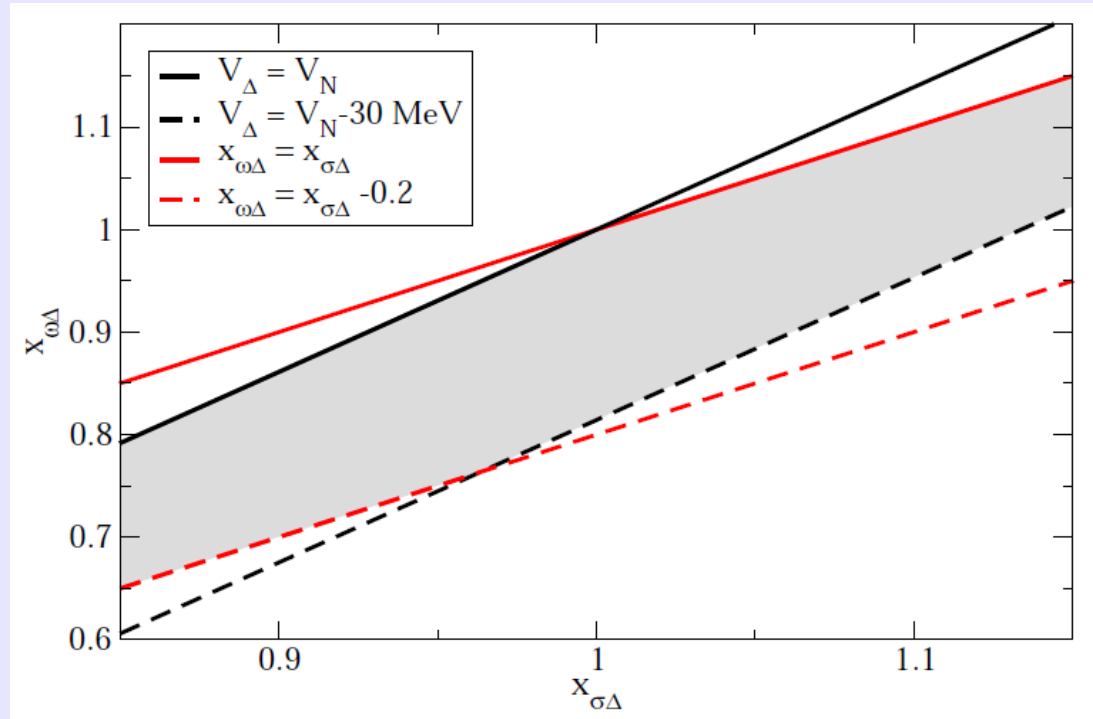


FIG. 4. Phenomenological nucleon-nucleus, solid line, and Δ nucleus, dashed line, momentum-dependent potentials for C.

This allows to constrain the free parameters within the RMF model. Notice: **coupling with ω mesons suppressed wrt the coupling with the σ meson.**

The coupling(ratio) with the ρ meson fixed to 1.



Implications for compact stars ?

To do: include the imaginary part of the delta self-energy in the equation of state calculations.

Simple estimates with a Breit-Wigner-like distribution. Critical density within the range of neutron stars central densities.

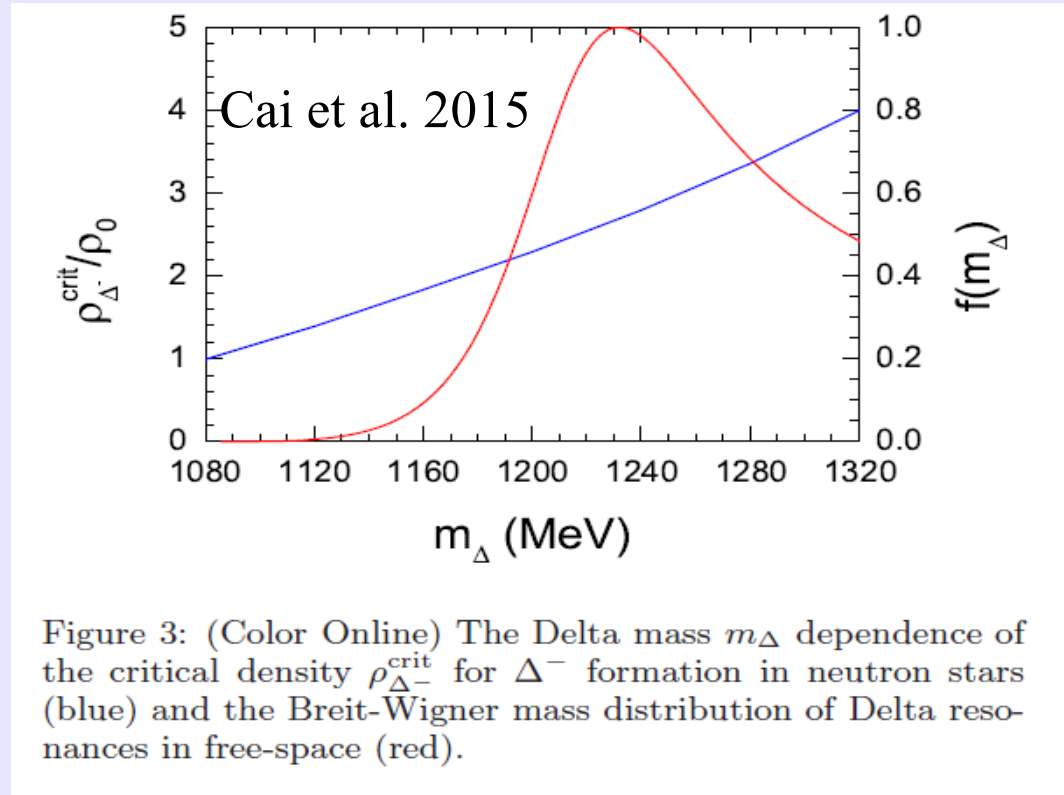


Figure 3: (Color Online) The Delta mass m_Δ dependence of the critical density $\rho_{\Delta^-}^{\text{crit}}$ for Δ^- formation in neutron stars (blue) and the Breit-Wigner mass distribution of Delta resonances in free-space (red).

$$f(m_\Delta) = \frac{1}{4} \frac{\Gamma^2(m_\Delta)}{(m_\Delta - m_\Delta^0)^2 + \Gamma^2(m_\Delta)/4}$$

Hyperons in compact stars

Few experimental data from hypernuclei: potential depths of Λ , Σ , Ξ allow to fix three parameters (usually the coupling with a scalar meson).

Within RMF:

(see Weissenborn, Chatterjee, Schaffner-Bielich 2012)

$$\begin{aligned}\mathcal{L} = & \sum_B \bar{\Psi}_B (i\gamma_\mu \partial^\mu - m_B + g_{\sigma B} \sigma - g_{\omega B} \gamma_\mu \omega^\mu - g_{\rho B} \gamma_\mu \mathbf{t}_B \cdot \boldsymbol{\rho}^\mu) \Psi_B \\ & + \frac{1}{2} (\partial_\mu \sigma \partial^\mu \sigma - m_\sigma^2 \sigma^2) - U(\sigma) + U(\omega) \\ & - \frac{1}{4} \omega_{\mu\nu} \omega^{\mu\nu} + \frac{1}{2} m_\omega^2 \omega_\mu \omega^\mu - \frac{1}{4} \rho_{\mu\nu} \cdot \rho^{\mu\nu} + \frac{1}{2} m_\rho^2 \rho_\mu \cdot \rho^\mu.\end{aligned}$$

$$\begin{aligned}\mathcal{L}_{YY} = & \sum_B \bar{\Psi}_B (g_{\sigma^* B} \sigma^* - g_{\phi B} \gamma_\mu \phi^\mu) \Psi_B \\ & + \frac{1}{2} (\partial_\mu \sigma^* \partial^\mu \sigma^* - m_{\sigma^*}^2 \sigma^{*2}) \\ & - \frac{1}{4} \phi_{\mu\nu} \phi^{\mu\nu} + \frac{1}{2} m_\phi^2 \phi_\mu \phi^\mu.\end{aligned}$$

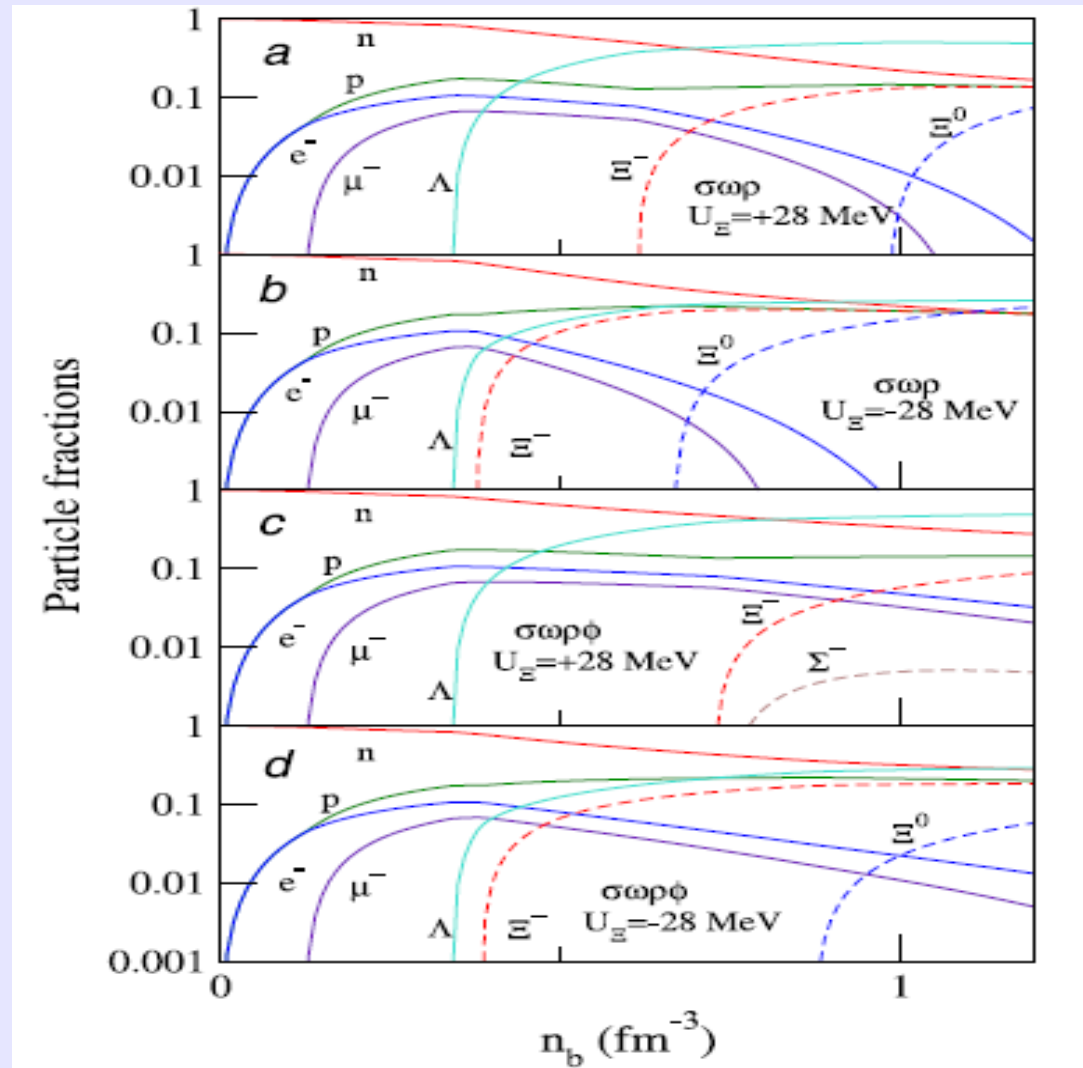
Additional
YY
interaction

$$\begin{aligned}\frac{1}{3} g_{\omega N} &= \frac{1}{2} g_{\omega \Lambda} = \frac{1}{2} g_{\omega \Sigma} = g_{\omega \Xi}, \\ g_{\rho N} &= \frac{1}{2} g_{\rho \Sigma} = g_{\rho \Xi}, \\ g_{\rho \Lambda} &= 0, \\ 2g_{\phi \Lambda} &= 2g_{\phi \Sigma} = g_{\phi \Xi} = -\frac{2\sqrt{2}}{3} g_{\omega N}.\end{aligned}$$

Couplings with vector mesons from flavor symmetry

Particle's fractions

Beta stable matter
(equilibrium with
respect to weak
interaction+charge
neutrality): large
isospin asymmetry and
large strangeness , very
different from the
nuclear matter
produced in heavy ions
collisions



Notice: hyperons appear at 2-3
times saturation density

The appearance of hyperons sizably softens the equation of state: reduced maximum mass

Introducing the ϕ meson to obtain YY repulsion allows to be marginally consistent with the astrophysical data.

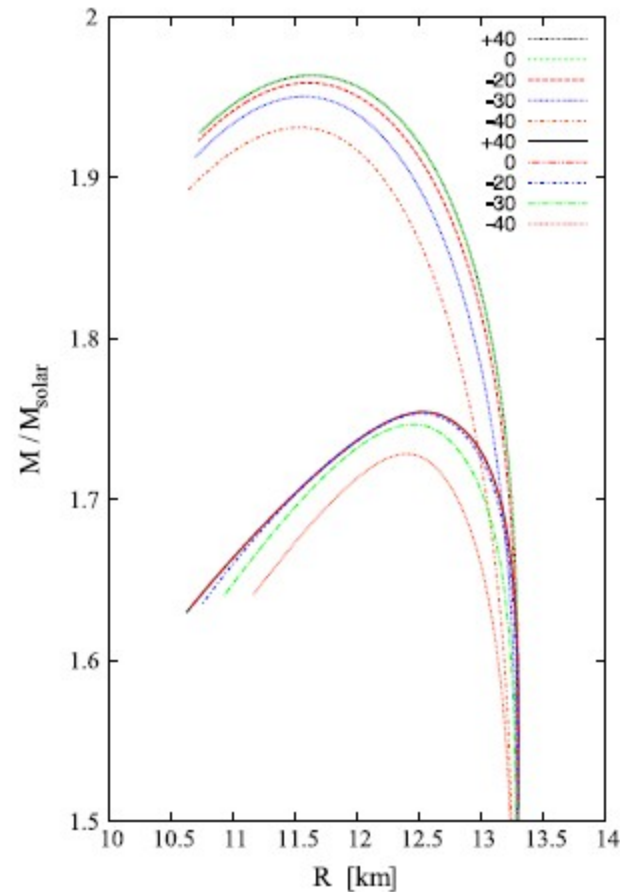


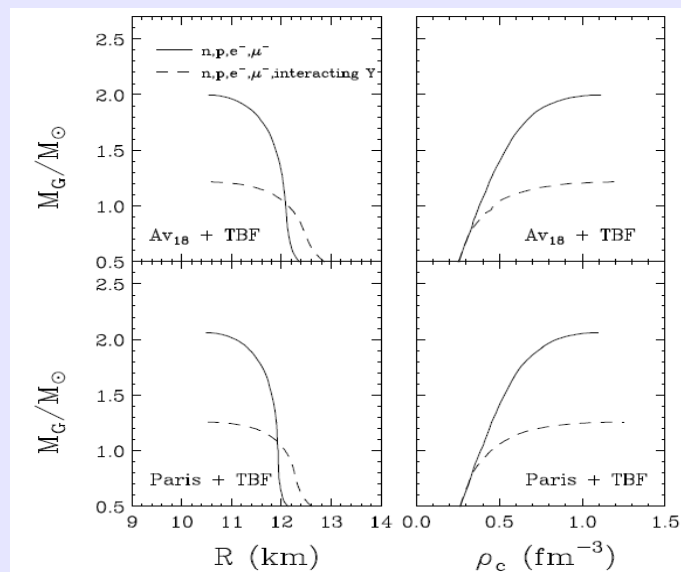
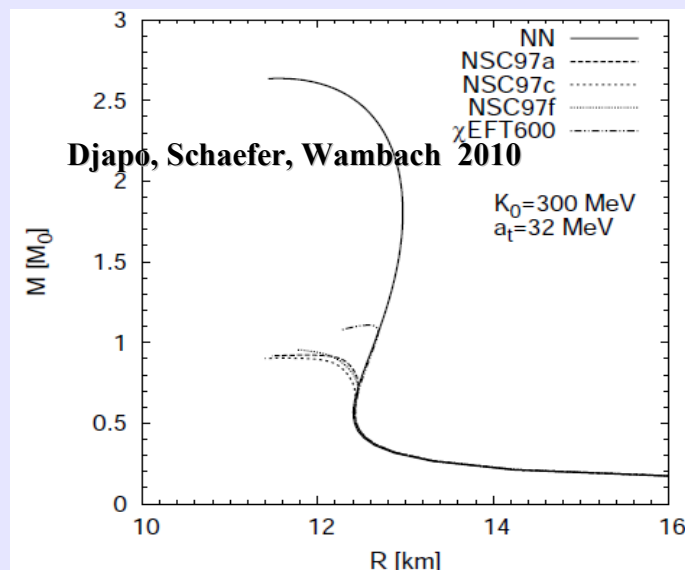
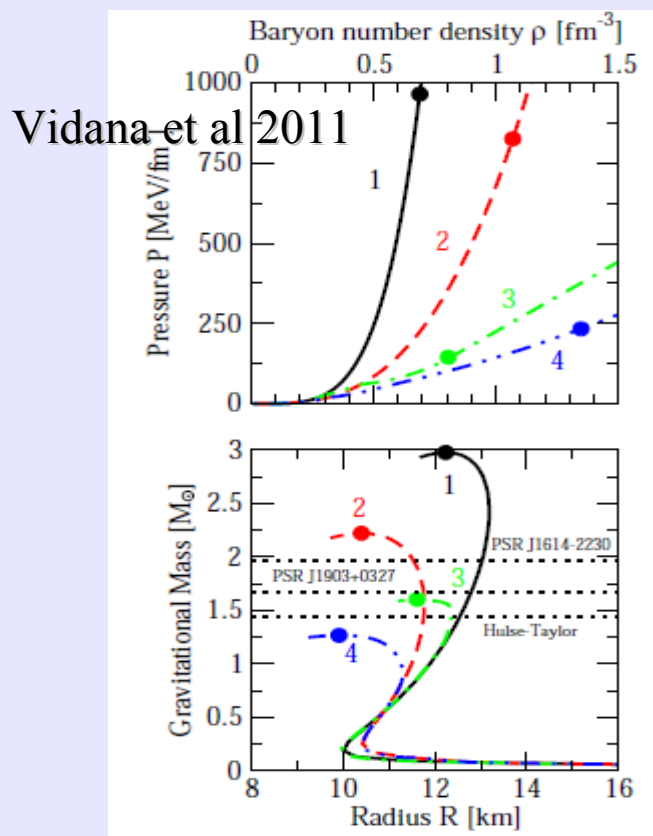
Fig. 2. Mass radius relations for neutron stars obtained with the EoS from Fig. 1. The variation of $U_{\Sigma}^{(N)}$ in “model $\sigma\omega\rho$ ” cannot account for the observed neutron star mass limit (lower branch), unless the ϕ meson is included in the model (upper branch).

... but: σ^* (to be interpreted as the $f_0(980)$) has not been included. Introducing this additional interaction would again reduce the maximum mass

... dramatic results in microscopic calculations

Hyperons puzzle: “...the treatment of hyperons in neutron stars is necessary and any approach to dense matter must address this issue.”

The solution is not just the “let's use only nucleons”



Baldo et al 1999

What about delta resonances?

Symmetry energy: the L parameter

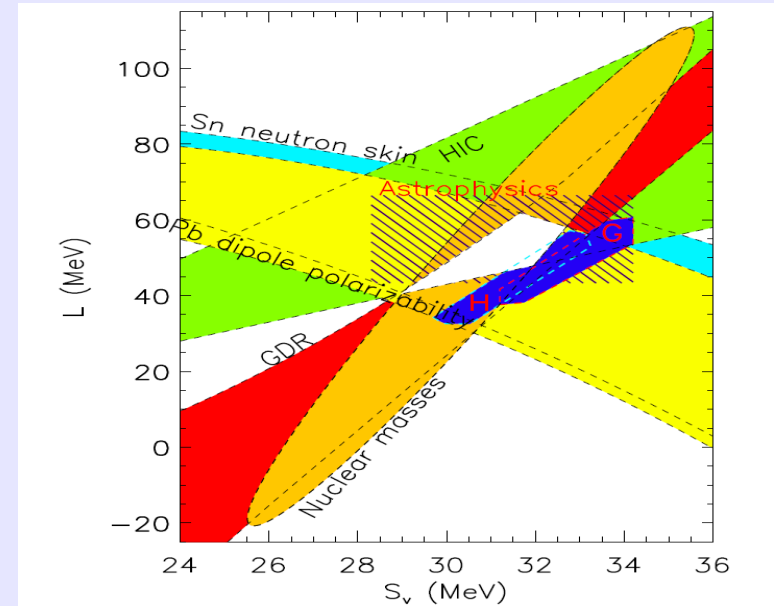
Symmetry energy and its density derivative

$$e(n, x) = e(n, 1/2) + S_2(n)(1 - 2x)^2 + \dots$$

$$S_v = S_2(n_s),$$

$$L = 3n_s(dS_2/dn)_{n_s}$$

Lattimer et al 2013



see also Horowitz et al 2013

Within the old Glendenning mean field parametrizations it was not possible to include this parameter as an additional constraint on nuclear matter

NEUTRON STARS ARE GIANT HYPERNUCLEI?¹

NORMAN K. GLENDENNING

Nuclear Science Division, Lawrence Berkeley Laboratory, University of California, Berkeley

Received 1984 March 28; accepted 1984 December 3

$$\mathcal{L} = \sum_B \bar{B}(i\gamma_\mu \partial^\mu - m_B + g_{\sigma B} \sigma - g_{\omega B} \gamma_\mu \omega^\mu)B$$

$$- g_\rho \rho_\mu 3 J_3^\mu + \mathcal{L}_\sigma^0 + \mathcal{L}_\omega^0 + \mathcal{L}_\rho^0 + \mathcal{L}_\pi^0 - U(\sigma)$$

$$U(\sigma) = [bm_N + c(g_\sigma \sigma)](g_\sigma \sigma)^3$$

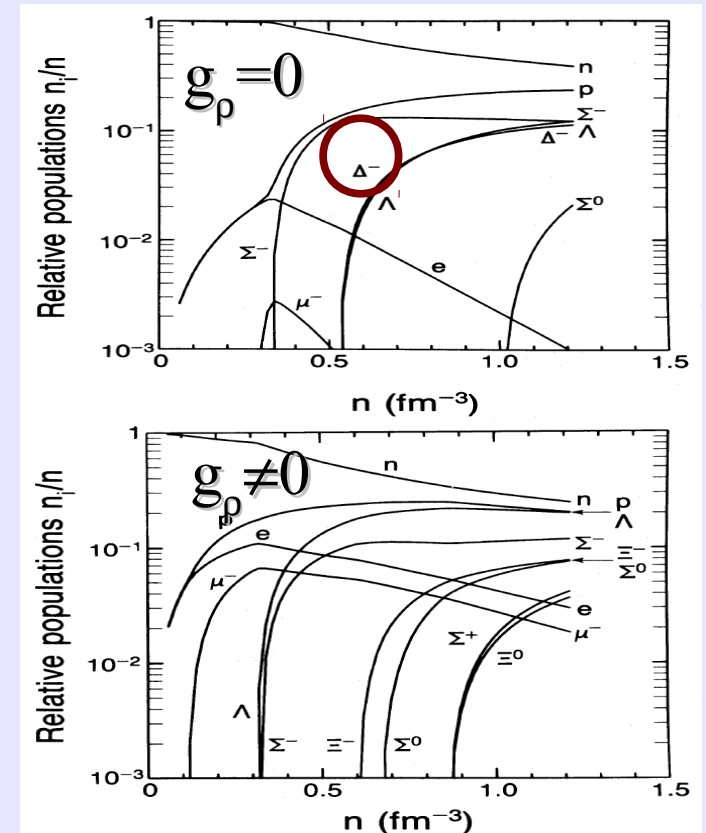
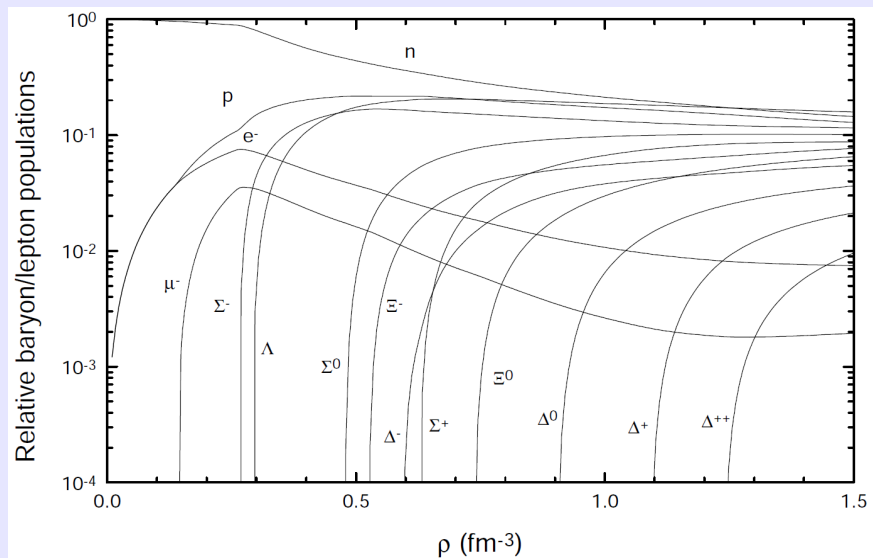
Only S_v could be fixed through g_ρ

... it turns out that in the GM1-2-3 parametrizations $L \sim 80$ MeV thus higher than the values indicated by the recent analysis of Lattimer & Lim.

Baryons thresholds equation

$$\mu_n - q_B \mu_e \geq g_{\omega B} \omega_0 + g_{\rho B} \rho_{03} I_{3B} + m_B - g_{\sigma B} \sigma$$

Disfavours the appearance of particles, such as Δ^- , with negative isospin charge. Δ^- could form in beta-stable matter only if g_ρ is set =0 (Glendenning 1984).

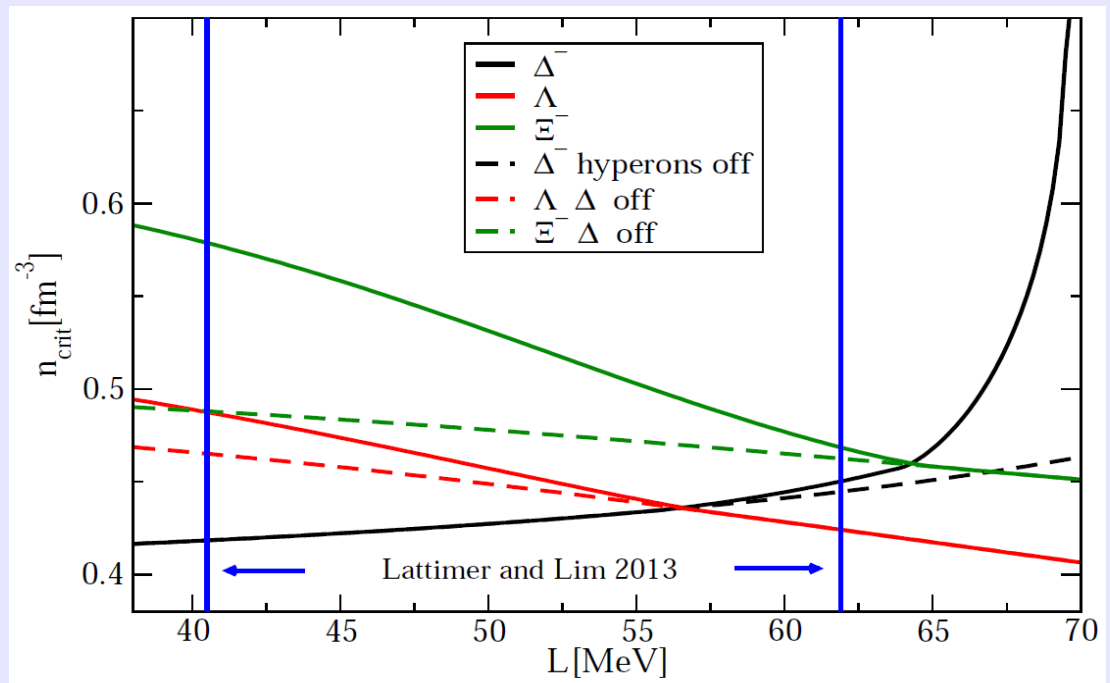


Δ^- easier to form in RHF calculations (see Huber et al 1998) due to the smaller value of g_ρ

A toy model: introduce a density dependence of g_ρ within the GM3 model (density dependence as in Typel et al 2009)

$$f_i(x) = \exp[-a_i(x - 1)]$$

The additional parameter “a” allow to fix L. Coupling ratios =1 for Δ , for hyperons potential depths and flavor symmetry (Schaffner 2000).



Different behaviour of the hyperons and Δ thresholds as functions of L:

$$g_{\rho n} \rho + \sqrt{k_{Fn}^2 + m_n^{*2}} + \mu_e = m_{\Delta-}^*$$

Punch line: for the range of L indicated by Lattimer & Lim, Δ appear already at 2-3 saturation density, thus comparable to the density of appearance of hyperons. If Δ form before hyperons, hyperons are shifted to higher densities (w.r.t. the case of no Δ)

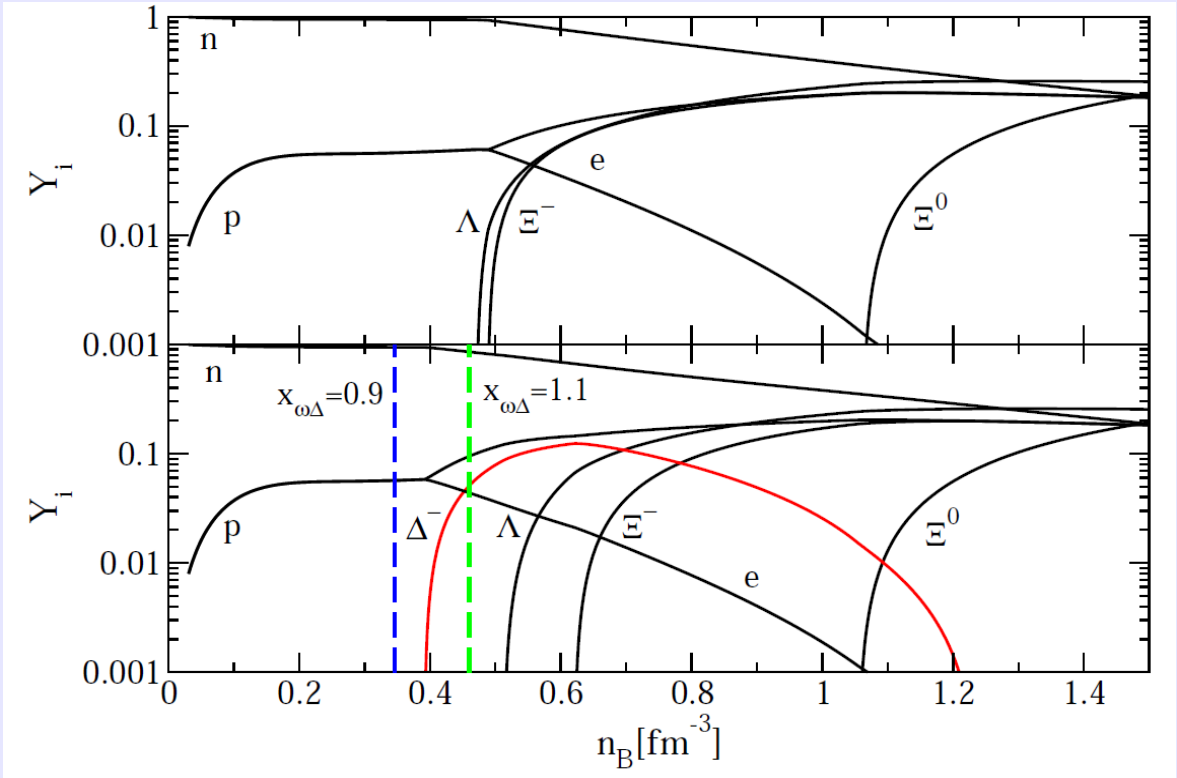
The recent SFHo model (Steiner et al 2013):
 additional terms added to better exploit the
 experimental information

$$\mathcal{L} = \bar{\Psi} \left[i \not{\partial} - g_\omega \not{\omega} - \frac{1}{2} g_\rho \not{\vec{\rho}} \cdot \vec{\tau} - M + g_\sigma \sigma - \frac{1}{2} e (1 + \tau_3) A \right] \Psi + \frac{1}{2} (\partial_\mu \sigma)^2 - V(\sigma) - \frac{1}{4} f_{\mu\nu} f^{\mu\nu} + \frac{1}{2} m_\omega^2 \omega^\mu \omega_\mu - \frac{1}{4} \vec{B}_{\mu\nu} \cdot \vec{B}^{\mu\nu} + \frac{1}{2} m_\rho^2 \vec{\rho}^\mu \cdot \vec{\rho}_\mu - \frac{1}{4} F_{\mu\nu} F^{\mu\nu} + \frac{\zeta}{24} g_\omega^4 (\omega^\mu \omega_\mu)^2 + \frac{\xi}{24} g_\rho^4 (\vec{\rho}^\mu \cdot \vec{\rho}_\mu)^2 + g_\rho^2 f(\sigma, \omega_\mu \omega^\mu) \vec{\rho}^\mu \cdot \vec{\rho}_\mu, \text{Steiner et al 2005}$$

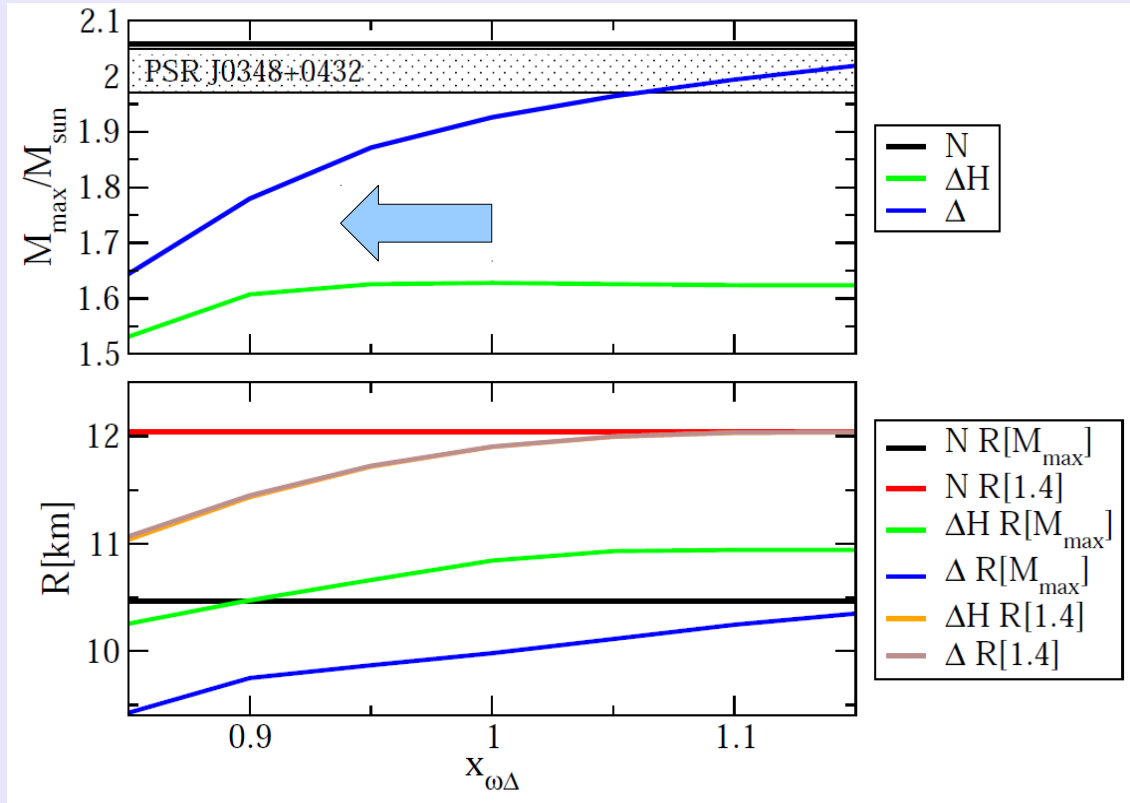
PROPERTIES AT SATURATION DENSITY AND NEUTRON STAR PROPERTIES FOR THE THE DIFFERENT EOSs UNDER INVESTIGATION. THE DEFINITION OF ALL THE QUANTITIES IS GIVEN IN THE TEXT.

EOS	n_B^0 [fm ⁻³]	E_0 [MeV]	K [MeV]	K' [MeV]	J [MeV]	L [MeV]	m_n^*/m_n -	m_p^*/m_p -	$R_{1.4}$ [km]	$M_{T=0,Max}$ [M _⊙]	$M_{s=4,Max}$ [M _⊙]
SFHo	0.1583	16.19	245.4	-467.8	31.57	47.10	0.7609	0.7606	11.88	2.059	2.27
SFHx	0.1602	16.16	238.8	-457.2	28.67	33.15	0.7179	0.7174	11.97	2.130	2.36
STOS(TM1)	0.1452	16.26	281.2	-285.3	36.89	110.79	0.6344	0.6344	14.56	2.23	2.62
HS(TM1)	0.1455	16.31	281.6	-286.5	36.95	110.99	0.6343	0.6338	13.84	2.21	2.59
HS(TMA)	0.1472	16.03	318.2	-572.2	30.66	90.14	0.6352	0.6347	14.44	2.02	2.48
HS(FSUGold)	0.1482	16.27	229.5	-523.9	32.56	60.43	0.6107	0.6102	12.52	1.74	2.34
LS(180)	0.1550	16.00	180.0	-450.7	28.61	73.82	1	1	12.16	1.84	2.02
LS(220)	0.1550	16.00	220.0	-411.2	28.61	73.82	1	1	12.62	2.06	2.14

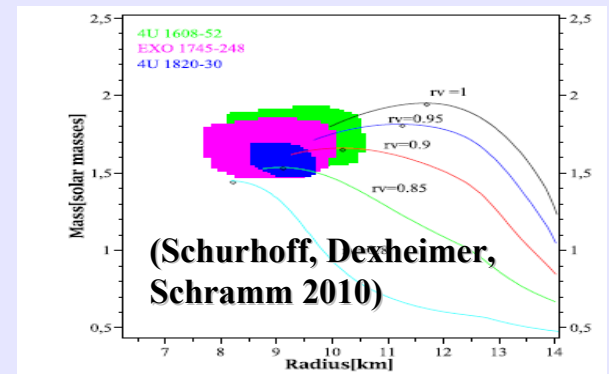
Introducing both
 hyperons and Δ in the
 SFHo model: Δ appear
 before hyperons even in
 the case of $x_{\omega\Delta} > 1$.



Maximum mass and radii: the maximum mass is significantly smaller than the measured ones. Also, very compact stellar configurations are possible.

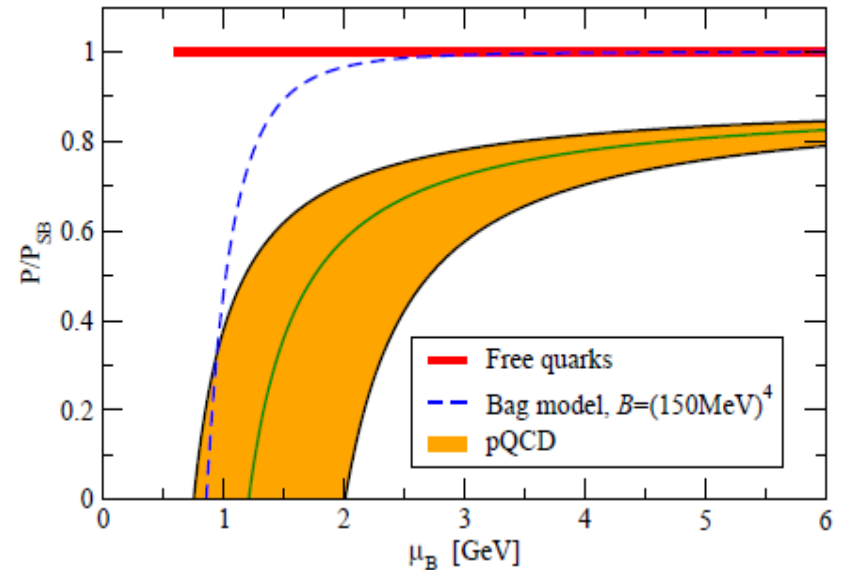
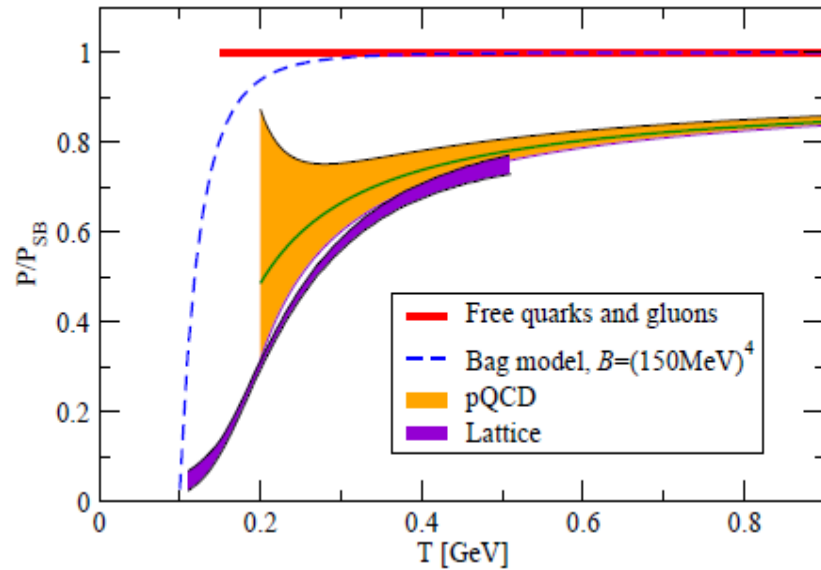


See also:



Punchline: beside the “hyperon puzzle” is there also a “delta isobars puzzle”?

pQCD results Kurkela et al.2014)



Case 1) *no neutrino cooling*:

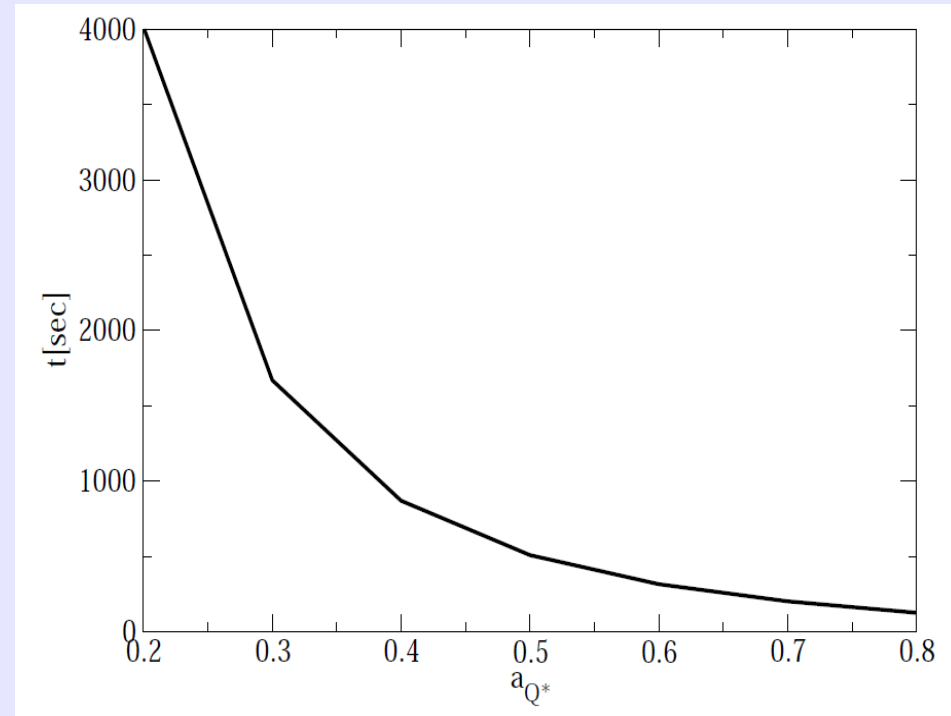
The new phase is produced at the pressure and enthalpy per baryon of the old phase: two equations which allow to determine the quark chemical potential and the temperature of the quark phase.

r_f : position of the flame front

$$\frac{dr_f}{dt} = v_{lf}(\mu_q, T)$$

$$r_f(0) \sim 9\text{km}$$

Time needed to complete the conversion of the hadronic star (upper limit since T is large),
long: cooling must be included



Case 2): *including cooling ... but in a very schematic way:*

-) Uniform temperature, black body emission from the neutrinosphere located at r_s (we have assumed that neutrinos decouple at the inner crust-outer crust interface)

$$\frac{dr_f}{dt} = v_{lf}(\mu_q, T)$$

$$C(T) \frac{dT}{dt} = -L(T) + 4\pi r_f^2 j(r_f, T) q(r_f, T)$$

$$L = 21/8 \sigma (T/K)^4 4\pi r_s^2$$

$$C = 2 \times 10^{39} M/M_\odot (T/10^9) \text{ erg/K}$$



Source of heat: energy released by the conversion

$v \sim 1/T^{5/6}$ the more material is converted the higher the temperature the slower the velocity. Self-regulating mechanism!